

# The role of emission reductions and the meteorological situation for air quality improvements during the COVID-19 lockdown period in Central Europe

Volker Matthias<sup>1</sup>, Markus Quante<sup>1</sup>, Jan A. Arndt<sup>1</sup>, Ronny Badeke<sup>1</sup>, Lea Fink<sup>1</sup>, Ronny Petrik<sup>1</sup>, Josefine Feldner<sup>1</sup>, Daniel Schwarzkopf<sup>1</sup>, Eliza-Maria Link<sup>1</sup>, Martin O.P. Ramacher<sup>1</sup>, Ralf Wedemann<sup>1</sup>

<sup>1</sup>Helmholtz-Zentrum Hereon, Max-Planck-Straße 1, 21502 Geesthacht, Germany

Correspondence to: Volker Matthias (volker.matthias@hereon.de)

**Abstract.** The lockdown measures taken to prevent a rapid spreading of the Corona virus in Europe in spring 2020 led to large emission reductions, particularly in road traffic and aviation. Atmospheric concentrations of NO<sub>2</sub> and PM<sub>2.5</sub> were mostly reduced when compared to observations taken for the same time period in previous years, however, concentration reductions may not only be caused by emission reductions but also by specific weather situations.

In order to identify the role of emission reductions and the meteorological situation for air quality improvements in Central Europe, the meteorology chemistry transport model system COSMO-CLM/CMAQ was applied to Europe for the period 1 January to 30 June 2020. Emission data for 2020 was extrapolated from most recent reported emission data and lockdown adjustment factors were computed from reported activity data changes, e.g. google mobility reports. Meteorological factors were investigated through additional simulations with meteorological data from previous years.

The results showed that lockdown effects varied significantly among countries and were most prominent for NO<sub>2</sub> concentrations in urban areas with two-weeks-average reductions up to 55% in the second half of March. Ozone concentrations were less strongly influenced (up to +/- 15%) and showed both increasing and decreasing concentrations due to lockdown measures. This depended strongly on the meteorological situation and on the NO<sub>x</sub>/VOC emission ratio. PM<sub>2.5</sub> revealed 2-12% reductions of two-weeks-average concentrations in March and April, which is much less than a different weather situation could cause. Unusually low PM<sub>2.5</sub> concentrations as observed in Northern Central Europe were only marginally caused by lockdown effects.

The lockdown can be seen as a big experiment about air quality improvements that can be achieved through drastic traffic emission reductions. From this investigation, it can be concluded that NO<sub>2</sub> concentrations can be largely reduced, but effects on annual average values are small when the measures last only a few weeks. Secondary pollutants like ozone and PM<sub>2.5</sub> depend more strongly on weather conditions and show a limited response to emission changes in single sectors.

## 1 Introduction

The global spread of the Corona virus since the start of 2020 resulted in unprecedented emission reductions caused by lockdown measures in many parts of the world. In Europe, significant reductions in road and air traffic as well as in industrial activities began between end of February and mid of March 2020. Emissions were heavily reduced

36 in short time, but then steadily increased again as lockdown measures were lifted step by step, until they reached  
37 approximately previous year levels in summer (Forster et al., 2020). However, this temporal emission behaviour  
38 varied from country to country and among the different emission sectors. Emission reductions between the second  
39 half of March and end of June 2020 were probably the largest in Europe since decades, in particular in traffic.  
40 From an air quality perspective, this can be regarded as a huge real world experiment about the effects of severe  
41 emission reductions on air pollutant concentrations and possible side effects of emission reduction measures, e.g.  
42 on secondary pollution formation.

43 Observational data at ground level and from satellite showed large, but regionally different reductions in NO<sub>2</sub>  
44 concentrations (e.g. Bauwens et al. (2020); Menut et al. (2020); Velders et al. (2021); Lonati and Riva (2021)). For  
45 particulate matter (PM), concentration reductions were less clear and not necessarily in line with the expectations  
46 that would follow the estimated emission reductions. Obviously, ~~also~~ weather conditions ~~also~~ have a significant  
47 impact on pollutant concentration levels, but despite the high number of publications that analyse COVID-19  
48 lockdown effects on air pollution, meteorological influences are mostly not taken into account properly (Gkatzelis  
49 et al., 2021). Wind direction determines strongly the advection of gases and aerosols from distant regions into the  
50 area of interest, higher wind speeds can activate additional emission sources like re-suspension of deposited  
51 particles, solar radiation affects photochemical reactions, and precipitation amounts control deposition. ~~In Central  
52 Europe, a period between mid of March and mid of April was very sunny and dry, both conditions that favour the  
53 formation of secondary pollutants like ozone and PM and that hamper particle deposition. On the other hand,  
54 advection of clean air from northern Europe influenced pollution levels in northern Central Europe in the  
55 beginning of April, as well.~~

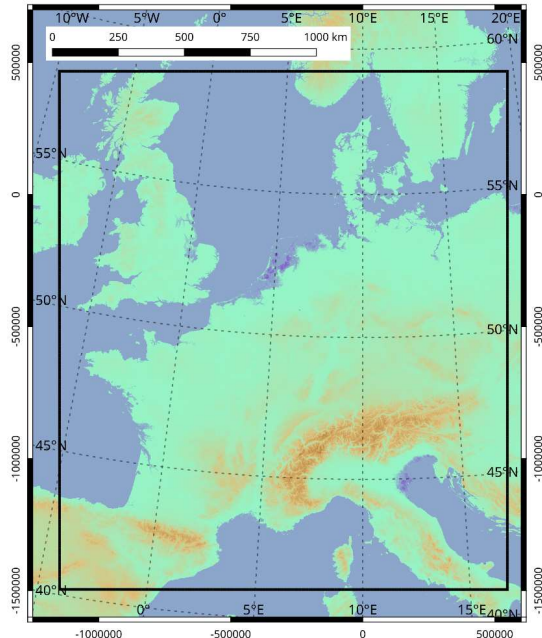
56 As has been pointed out in recent publications about the effect of COVID lockdown emission reductions on air  
57 pollutant concentrations (e.g. Menut et al. (2020); Velders et al. (2021)), the relationship between emissions and  
58 concentrations is not necessarily straightforward and easy to explain. A simple comparison between before and  
59 after lockdown concentrations neglects seasonal and weather effects. A similar argument holds for comparisons  
60 with the same week of the previous year. While seasonal effects are considered in this case, the weather situation  
61 might still be very different. In addition, technology or economically driven emission changes from one year to  
62 another are not taken into account. Chemistry transport models and sophisticated emission models can help in  
63 disentangling the relationships between emissions, meteorology, and concentration levels. In addition, they can  
64 quantify the contribution of different source sectors and investigate effects of reduced concentrations of specific  
65 pollutants on the formation of other secondary species. For example, it has been discussed by Kroll et al. (2020)  
66 and Huang et al. (2020) that lower NO emissions might lead to higher ozone concentrations and a higher potential  
67 for the oxidation of organics, which might result in increased secondary organic aerosol (SOA) formation. In fact,  
68 Amouei Torkmahalleh et al. (2021) analysed observed NO<sub>2</sub> and O<sub>3</sub> concentrations in numerous cities around the  
69 world and report increased ozone in urban environments. However, depending on the NO<sub>x</sub>/VOC emission ratios  
70 and the meteorological situation, the effects might differ from place to place (see e.g. Mertens et al. (2021)).

71 To quantify the effects of the lockdown measure on ambient concentrations, these need to be separated from other  
72 sources of influence which predominantly are assumed to be the meteorological conditions. For Europe, Menut  
73 et al. (2020) assessed the influence of lockdown measures on air quality without the biases of meteorological  
74 conditions in an ad-hoc modelling study for March 2020. They compared a reference model run with 2017  
75 emission data for Europe to a lockdown run with estimated emission reductions. Both runs were based on the

76 same meteorological fields. ~~Considerable d~~Decreases in NO<sub>2</sub> concentrations ~~ranging from –30% to –50% in all~~  
77 ~~western European countries~~ due to the lockdown measures alone have been found. The effect on fine particle  
78 concentrations has been comparably less pronounced (–5 to –15%). Sharma et al. (2020) performed a similar  
79 study for India. ~~they reported a remarkable –Around 43%, 31%, 10%, and 18% decreases in PM<sub>2.5</sub>, PM<sub>10</sub>, CO,~~  
80 ~~and NO<sub>2</sub> in India were observed during the lockdown period compared to previous years. While, there were 17%~~  
81 ~~increase in O<sub>3</sub> and negligible changes in SO<sub>2</sub>.~~ With focus on the Netherlands, Velders et al. (2021) used a machine  
82 learning (ML) algorithm (~~Random forest~~) to remove the effects due to meteorological variability on pollutant  
83 concentrations ~~and –Concentrations that were measured before and during the lockdown period are compared~~  
84 ~~with the “expected” concentrations during this period, according to the ML algorithm and the differences are~~  
85 ~~ascribed to the lockdown measures. The authors also applied chemical transport modelling to assess the question~~  
86 ~~of separating the effects.~~ They concluded that the unusual 2020 meteorology in the Netherlands led to decreased  
87 PM<sub>10</sub> and PM<sub>2.5</sub> concentrations ~~by about 8% and 10%, respectively,~~ but the NO<sub>x</sub>, NO<sub>2</sub>, and O<sub>3</sub> concentrations  
88 were not affected. In a study addressing the air quality during the lockdown period in Milan Collivignarelli et al.  
89 (2020) ~~used a different procedure based on observations, only, aiming to eliminated~~ the influence of weather  
90 phenomena on the air quality. ~~To do so, they by identifying~~ a meteorological reference period ~~in the same year~~  
91 ~~around the lockdown phase. About two weeks in February (7th to 20th) were considered suitable to serve as a~~  
92 ~~control time segment, for which gas and particle concentrations were used to quantify the lockdown effects.~~ Using  
93 machine-learning (ML) models fed by meteorological data ~~along with other time features.~~ Petetin et al. (2020)  
94 estimated the NO<sub>2</sub> mixing ratios for Spain that would have been observed ~~in the absence of the lockdown. So-~~  
95 ~~called meteorology-normalized NO<sub>2</sub> reductions induced by the lockdown measures were quantified by comparing~~  
96 ~~the estimated business-as-usual values with the observed NO<sub>2</sub> mixing ratios.~~ It was found that the lockdown  
97 measures were responsible for a 50% reduction in NO<sub>2</sub> levels ~~on average over all Spanish provinces and islands~~  
98 ~~during the period from 14 March to 23 April 2020. Additionally~~ Goldberg et al. (2020) ~~showed that accounting for~~  
99 ~~meteorological influences is important when satellite data is used to estimate the drops in columnar NO<sub>2</sub> in the~~  
100 ~~United States. And,~~ van Heerwaarden et al. (2021) used ground based and satellite observations in combination  
101 with radiative transfer modelling to disentangle meteorological effects and those of aerosol emissions ~~reduction~~  
102 ~~and reduced contrails on observed record irradiance in Western Europe.~~ They concluded that lockdown measures  
103 were far less important for the irradiance record than the exceptionally dry and particularly cloud-free weather.  
104 In this paper we present results derived with the COSMO-CLM/CMAQ model system together with a highly  
105 modular emission model to quantify the contribution of the estimated emission reductions on the concentrations  
106 of NO<sub>2</sub>, O<sub>3</sub> and PM<sub>2.5</sub> in Central Europe and to separate the contribution of emission changes from those caused  
107 by distinct weather patterns. CMAQ was fed with updated emission data for the year 2020, including time profiles  
108 for sectors and countries that approximate the lockdown emission reductions. Chemistry transport model  
109 simulations were performed for January – June 2020. The effects of distinct weather patterns on the effects of  
110 emission reductions on pollutant concentrations were investigated through additional simulations with  
111 meteorological conditions for the same time period in recent previous years with very different weather conditions.  
112 The results allow for an interpretation of the observed concentration reductions when compared to previous years.  
113 It also gives a range of possible concentration changes resulting from the same emission reductions.

Formatiert: Tiefgestellt

114 **2 Model simulations**



115 **Figure 1: Inner domain of the CMAQ model (black line) along with the coordinates of the CMAQ projection (values**  
116 **outside the zebra frame)**  
117

118 This study focuses on the effects of emission reductions during the lockdown in Central Europe in spring and  
119 early summer 2020. While emission changes were considered for entire Europe, the main area under investigation  
120 w.r.t. effects on concentrations covers the most populated regions in Central Europe (Fig. 1), only. This restriction  
121 was applied for the sake of a higher resolution and for allowing a reasonable interpretation of meteorological  
122 impacts. The Community Multi-scale Air Quality Model (CMAQ) (Byun and Schere, 2006; Byun and Ching,  
123 1999) version 5.2 was used with the carbon bond 5 (CB05) photochemical mechanism (CB05tucl) (Kelly et al.,  
124 2010) and the AE6 aerosol mechanism. The model was run for 2020 with a spin-up time of 2 weeks in 2019 to  
125 avoid the influence of initial conditions on the modelled atmospheric concentrations. CMAQ was set up on a 36  
126 x 36 km<sup>2</sup> grid for entire Europe and for a one-way nested 9 x 9 km<sup>2</sup> grid for Central Europe, see Fig. 1. The vertical  
127 model extent comprises 30 layers from the model surface up to the 100 hPa pressure level. Twenty of these layers  
128 are below approx. 2000 m, and the lowest layer has a height of 36 m.

129 Chemical boundary conditions for the outer model domain were taken from the IFS-CAMS analysis (Inness et al.,  
130 2019b) available from the MARS archive at ECMWF and the Copernicus Atmosphere Monitoring Service  
131 Atmosphere Data Store (Inness et al., 2019a). Particle and gas concentration fields of the Global Analysis and  
132 Forecast are provided on a T511 spectral grid with 137 vertical levels. [Emission changes caused by lockdown](#)  
133 [measures are not considered in this data set.](#) The IFS-CAMS data were temporally and spatially remapped onto  
134 the boundary of the CMAQ domain. Finally, a unit conversion and a transformation of the chemical species from  
135 IFS-CAMS to CMAQ were applied.

Formatiert: Hochgestellt  
Formatiert: Hochgestellt

136 Meteorological data for the CMAQ model were provided by a simulation of the COSMO model (Baldauf et al.,  
137 2011;Doms et al., 2011;Doms and Schättler, 2002) applying the version COSMO5-CLM16 (climate mode  
138 (Rockel et al., 2008)). To simulate the radiative transfer as realistic as possible, an extension of the COSMO model  
139 for the MACv2 transient aerosol climatology was used. The soil was initialized taking the data from a 40 year  
140 simulation with the COSMO model. Then, the atmospheric simulations were performed for the period 1  
141 September 2019 to 30 June 2020 using the MERRA2 Global reanalysis (Gelaro et al., 2017) as initial and lateral  
142 boundary conditions. The same was done for the periods 1 September 2015 to 30 June 2016 and 1 Sep 2017 to 30  
143 June 2018. To ensure that the atmospheric fields in the transient model integration are close to the observations  
144 over the whole period of 10 months, a nudging technique was used as described in Petrik et al. (2021). The reader  
145 is referred to this publication to find more information about the setup of the atmospheric model (setup 'CCLM-  
146 oF-SN').

147 CMAQ simulations were performed with emissions as they could be expected for 2020 without any lockdown  
148 measures and with another emission data set that was modified according to reported changes in traffic and  
149 industrial activities. The latter is regarded as the emission data set that **best** reproduces real world emissions during  
150 the first COVID-19 lockdown phase in 2020-**best**. In the following we will refer to this simulation as the COV  
151 case, while the simulations with expected emissions without lockdown is referred to as the noCOV case. The  
152 difference between the simulated pollutant concentrations for the two cases represents the COVID-19 lockdown  
153 effects on air quality. A detailed description of the emission data construction is given in the next section.  
154 Additional model simulations with meteorological conditions for the years 2016 and 2018 have been performed  
155 with CMAQ using the same 2020 emission data sets.

### 156 3 Emission data

#### 157 3.1 Basic emissions 2020, noCOV case

158 Emissions are based on the CAMS-REGAP-EU version 3.1 available at the ECCAD website  
159 (<https://permalink.aeris-data.fr/CAMS-REG-AP>). The dataset comprises annual totals for anthropogenic  
160 emissions in 13 GNFR sectors (Granier et al., 2019). The most recent data set was for 2016. For this study, the  
161 emission data was extrapolated to the year 2020 based on the temporal emission development in previous years.  
162 For the application in the CMAQ model the data was re-gridded and vertically and temporally redistributed.  
163 Additionally, in order to investigate the effects of lockdown measures on the emissions, sector and country specific  
164 temporal profiles of lockdown effects were applied. The data preparation was done with a modular toolbox for  
165 emission calculation, the Highly Modular Emission MOdel (HiMEMO), currently developed at Helmholtz-  
166 Zentrum Hereon. The framework is built in the R programming language, using the libraries netcdf, proj4, sp,  
167 raster and their dependencies.

168 HiMEMO was run with gridded emission data from the CAMS inventory for 2016 in a spatial resolution of  $0.05^\circ$   
169  $\times 0.1^\circ$ . The inventory contains gridded annual emissions for chemical species groups, i.e.  $\text{NO}_x$ , NMVOC, CO,  
170  $\text{NH}_3$ ,  $\text{CH}_4$ ,  $\text{SO}_2$ ,  $\text{PM}_{2.5}$  and  $\text{PM}_{10}$ . Several of these chemical groups need to be split into chemical components, or  
171 sub-groups of species according to the CB05 chemical mechanism used by CMAQ. The  $\text{NO}_x$  split was done by  
172 applying a  $\text{NO}/\text{NO}_2$  ratio of 90/10 for traffic, a ratio of 92/8 for shipping and 95/5 for all other sectors. Land based  
173 NMVOC emissions were split for individual sectors [according to a split provided by TNO \(J. Kuenen, pers.](#)

Formatiert: Tiefgestellt

Formatiert: Tiefgestellt

174 [communication](#)). PM was split as described by Bieser et al. (2010) for the SMOKE for Europe emission model.  
175 All other species in the CAMS-REGAP-EUP inventory were directly transferred to CMAQ.  
176 Vertical emission distributions per sector follow Bieser et al. (2011). The vertical distribution for the shipping  
177 sector was treated differently for land and ocean-going ships, the latter being emitted in altitudes up to 100 m. The  
178 temporal profiles follow those provided by TNO (Denier van der Gon et al. (2011), also described in Matthias et  
179 al. (2018)).  
180 Biogenic emissions of VOCs (BVOCs) and NO were calculated with the Model of Emissions of Gases and  
181 Aerosols from Nature (MEGAN) (Guenther et al., 2012). Version 3 of MEGAN (Guenther et al., 2020) was used  
182 in this study, it was driven by preprocessed meteorological data for CMAQ as described above. Vegetation data  
183 tables were downloaded from the MEGAN website and not further modified for this study. Leaf area index (LAI)  
184 data was taken from GEOV1 products (SPOT/PROBA V LAI1) as an alternative input for MEGAN3 (Baret et  
185 al., 2013).  
186 The annual [emission](#) data for 2016 were extrapolated to 2020 for each national emission sector according to the  
187 Gridded Nomenclature For Reporting (GNFR) in order to produce expected emissions for 2020 without lockdown  
188 effects. The starting point were the time series data of yearly totals for the pollutants BC, CO, NH<sub>3</sub>, NMVOC,  
189 NO<sub>x</sub>, PM<sub>10</sub>, PM<sub>2.5</sub> and SO<sub>2</sub>, which are provided by the EMEP centre on emission inventories and projections  
190 (EMEP/CEIP 2020 Present state of emission data; [https://www.ceip.at/webdab-emission-database/reported-](https://www.ceip.at/webdab-emission-database/reported-emissiondata)  
191 [emissiondata](https://www.ceip.at/webdab-emission-database/reported-emissiondata)). Using the time series data, a mean annual change rate for emissions (CE, in %) was derived for  
192 each pollutant, sector and country, separately. The projection of the 2016 emissions to the year 2020 was realized  
193 through a projection factor  $PF=1+ CE/100*(2020-2016)$ . Using a mean change rate based on the development of  
194 emissions within the 3 years 2017-2019 (method 1), PF could be very large (more than 2) for some countries and  
195 sectors. This can result from large changes and fluctuating time series of the yearly emissions. In order to avoid  
196 very large and presumably erroneous emission changes between 2016 and 2020, a maximum allowed annual  
197 change rate was introduced. If the CE was larger than 10%, a modified CE was computed by considering the entire  
198 time series of annual emissions, but not more than ten years (method 2). If there still was a CE of more than 10%,  
199 we limited it to a maximum change of  $\pm 10\%$ . Regarding the shipping sector, no changes were assumed between  
200 the years 2016 and 2020.

### 201 3.2 Lockdown effects, COV case

202 For the lockdown scenario, we adjusted national emissions from the following GNFR sectors: A\_PublicPower,  
203 B\_Industry, F\_RoadTransport, G\_Shipping and H\_Aviation. Lockdown emission reduction functions, here called  
204 Lockdown Adjustment Factors (LAF) were calculated based on published data sources that resemble the effects  
205 of lockdown measures on a daily basis. LAFs were derived for 42 European countries and two sea basins, the  
206 North Sea and the Baltic Sea.

207 The datasets used for the construction of the ~~modification-functions~~LAFs are described in the following. If the  
208 input data was not available for an individual country, data from a neighbouring country was used to estimate the  
209 reduction. A table showing the data availability per sector and country is given in the appendix (Table A1). The  
210 ~~modification-functions~~LAFs are applied to all species, heights and time steps of the anthropogenic emission  
211 dataset for 2020.

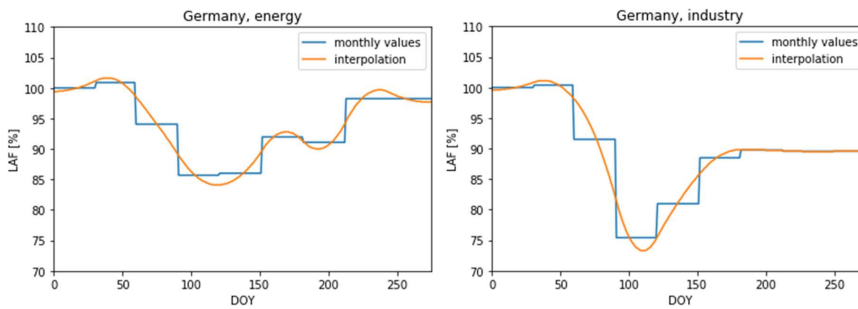
#### 212 A\_PublicPower and B\_Industry

Formatiert: Tiefgestellt

Formatiert: Tiefgestellt

213 Eurostat data ([https://ec.europa.eu/eurostat/databrowser/view/sts\\_inpr\\_m/default/bar?lang=en](https://ec.europa.eu/eurostat/databrowser/view/sts_inpr_m/default/bar?lang=en)) was used to  
214 account for changes in the sectors A\_PublicPower and B\_Industry.

215 The energy data provided there comprise monthly information on the volume index of production for electricity,  
216 gas, steam and air conditioning supply. They are available for 35 countries in Europe. The industry data comprise  
217 monthly information on the volume index of production for mining and quarrying; manufacturing; electricity, gas,  
218 steam and air conditioning supply and construction and are available for 20 countries in Europe. The indices are  
219 based on an index value of 2015. However, since we want to use them to evaluate the lockdown period, we  
220 normalized the changes based on the January 2020 value. The data are given in a monthly resolution, however,  
221 for many countries in Europe the lockdown started in mid of March. Therefore, a piecewise cubic spline  
222 interpolation procedure was applied to derive daily lockdown adjustment factors while still maintaining the  
223 monthly values. Examples are given for both sectors in Germany in Fig. 2.



224

225 **Fig. 2: Examples for monthly values and interpolated functions for Lockdown Adjustment Factors (in %) for the**  
226 **sectors A\_PublicPower and B\_Industry in Germany.**

### 227 F\_RoadTransport

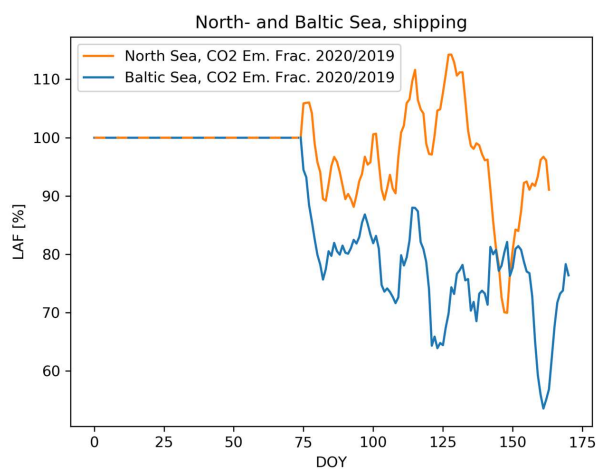
228 Google Mobility Reports (<https://www.google.com/covid19/mobility/>) deliver daily percentage change of visits  
229 in different areas (e.g. residential, transit, recreation, work places). The reference value is the median of the  
230 corresponding weekday between 3rd of January and 6th of February 2020. We use Google Mobility Reports for  
231 transit on a national level to account for the changes in road traffic emissions. Through this method, reduced traffic  
232 on national holidays, e.g. around Easter and 1 May are considered as well, however, vehicle types cannot be  
233 distinguished.

### 234 G\_Shipping

235 To derive scaling factors that account for ship traffic and emission reductions in this sector, bottom-up ship  
236 emission inventories were created with the HiMOSES ship emission model (Schwarzkopf et al., 2021) using  
237 Automatic Identification System (AIS) data for 2019 and 2020 covering the German Bight and the Western Baltic  
238 Sea. The data was recorded in Bremerhaven and Kiel by the German Federal Maritime and Hydrographic Agency  
239 (BSH). A 7-days rolling mean filter was applied to the calculated CO<sub>2</sub> emission ratios (Fig. 3). On average,  
240 the data revealed a slight reduction of ship traffic in the North Sea area by approx. 10%. For the Baltic Sea traffic  
241 reductions were clearly visible with a downward trend from March until mid of June that could be mainly

Formatiert: Tiefgestellt

242 attributed to Roll-on/Roll-off (RoRo) ships and passenger ships. For the first 75 days of the year until 15 March  
243 2020 no reductions were applied, afterwards daily LAF were used similar to the approach for road traffic. LAFs  
244 for the North Sea were also applied for the Mediterranean Sea, those for the Baltic Sea were also applied to inland  
245 shipping. The reasoning behind this is that shipping in the Mediterranean is mostly international cargo transport,  
246 similar to the North Sea, and inland navigation is connected to short range transport, similar to the Baltic Sea. As  
247 can be seen in Fig.3 relative increases in shipping emissions might also occur during limited time.



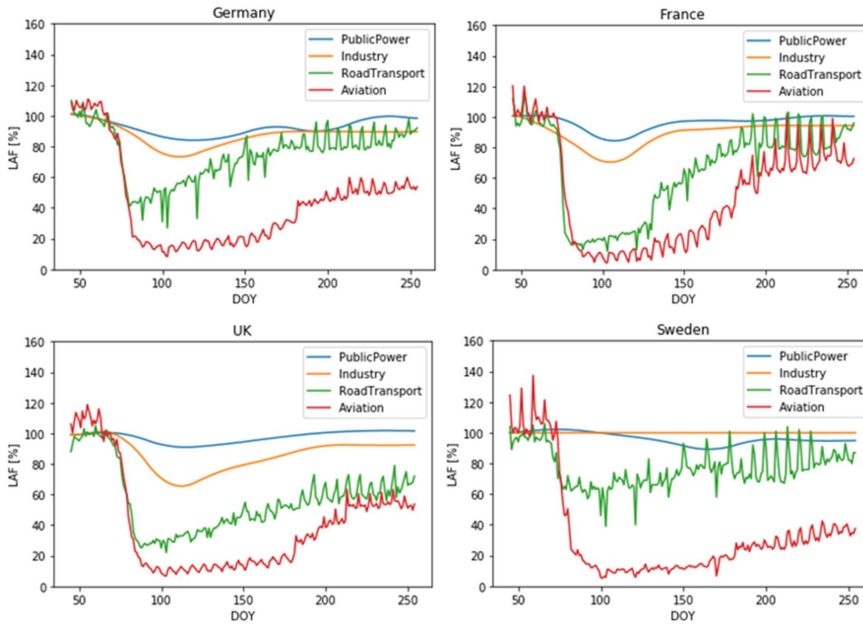
248  
249 **Fig 3: Lockdown adjustment factors created from the seven days rolling mean ratios of CO2 emissions from shipping**  
250 **in 2020 relative to 2019. Until day 75 (15 March) no changes and a LAF of 1 was assumed.**

### 251 H\_Aviation

252 Airport traffic total arrivals and departures data from Eurocontrol (<https://ansperformance.eu/data>) were used to  
253 account for emission changes in the aviation sector. We applied a reduction based on a weekday mean from 3  
254 January 2020 until 6 February 2020, similar to Google mobility data. Daily values for 42 European countries are  
255 available. The relative reductions in this sector were most pronounced, reaching -90% in March and April and a  
256 slower recovery than the other sectors.  
257



258 Sector Comparison



259

260

261 Fig. 4: LAFs for Germany (a), France (b), United Kingdom (c) and Sweden (d) for the sectors: A\_PublicPower,  
 262 B\_Industry, F\_RoadTransport, and H\_Aviation

263 LAFs for Germany, France, UK and Sweden are exemplarily shown in Figure 4. Huge emission reductions in  
 264 road traffic and air traffic between 10 and 20 March (day of the year (DOY) 70-80) can clearly be seen. Public  
 265 power and industry, on the other hand, show much smaller reductions (10-30%) and almost reach previous year  
 266 levels until the end of June. At the same time in France and Germany, road traffic was back to 90% of the previous  
 267 year, however in the UK and in Sweden 20-40% reductions were still visible in the activity data. Comparisons  
 268 of country-specific LAFs for the sectors F\_RoadTransport, and H\_Aviation are given in the supplement (Fig. A1  
 269 and A2).

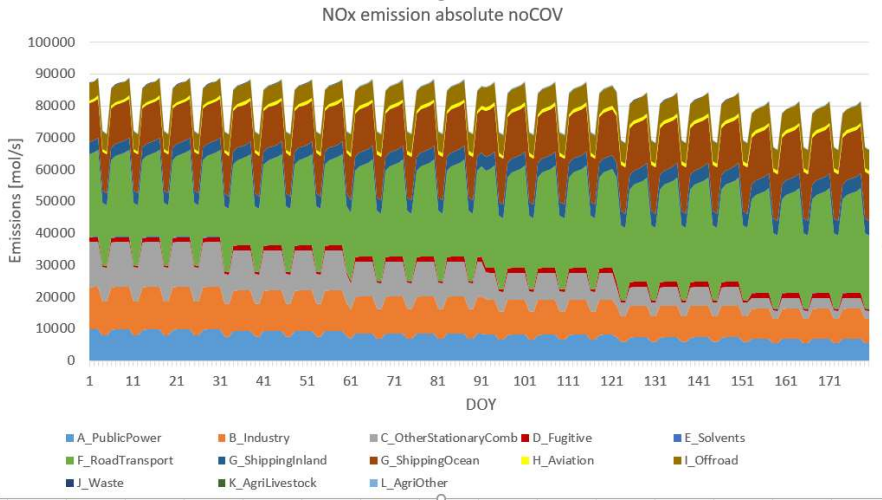
270 Figure 5 presents total daily  $\text{NO}_x$  emissions in the entire Central European domain (see Fig. 1) for the time period  
 271 from 1 January to 30 June 2020 for the COV and the noCOV case separated by GNFR sectors. Road transport is  
 272 the most important emission sector with approx. 20 to 30%, followed by ocean shipping, other stationary  
 273 combustion, industry and public power, which all have similar contributions of approx. 10%. Combustion shows  
 274 a clear decline towards the summer months due to the fact that domestic heating is mainly necessary in winter.  
 275 Reductions caused by the lockdown stem mostly from the road transport sector, with a strong drop in emissions  
 276 starting around DOY day 75 (15 March). The aviation sector, which experienced the strongest relative drop in  
 277 emissions during the lockdown, does not play a major role for the overall emission of  $\text{NO}_x$ . However, it might be  
 278 important near airports and in the upper troposphere. Overall,  $\text{NO}_x$  emissions in Central Europe dropped by around  
 279 25000 mol/s (approx. 4 kt/h, when given as  $\text{NO}_2$ ) during the strictest lockdown period in late March and early  
 280 April. This corresponds to a relative drop of around -30% (Fig. 5).

Formatiert: Tiefgestellt

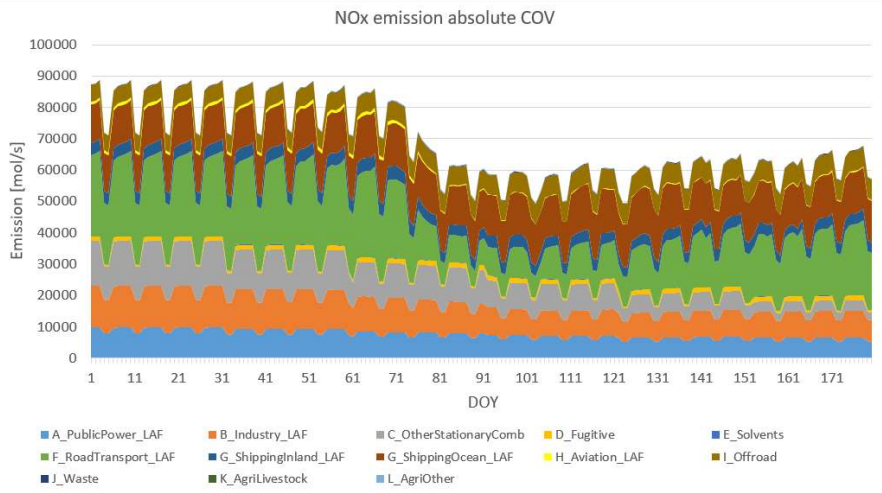
Formatiert: Tiefgestellt

Formatiert: Tiefgestellt

281



282



283

284 **Fig.5: Daily average values for sector separated NOx emissions summarized over the entire Central European model**  
285 **domain for the noCOV and the COV case (with LAF).**

286 **4 Observational data**

287 We focus our analysis on the most important air pollutants for human health, namely NO<sub>2</sub>, O<sub>3</sub> and PM<sub>2.5</sub>. In this  
288 chapter, first the meteorological situation between 1 January and 30 June 2020 is analysed. Afterwards,  
289 observational air quality data at six selected measurement stations within the EEA network  
290 (<https://www.eionet.europa.eu/countries/index>) are presented and discussed.

291 **4.1 Meteorological situation**

292 During the lockdown period in spring 2020 large parts of the region of interest experienced exceptional weather,  
293 ~~what~~ that is assumed to have a strong influence on concentrations of some of the pollutants in focus.

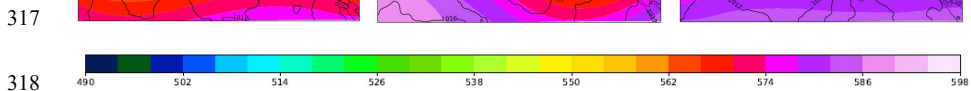
294 The weather conditions during the first half of the year 2020 show strong variations across the months and a  
295 different character in the northern part of our model domain compared to more southern regions like the Po Valley.

296 While in the North February was extremely wet and windy (south-westerly direction), the second half of March  
297 and April were very dry and sunny. Thus for meteorological reasons a comparison of pre-lockdown pollutant  
298 concentrations with those during the lockdown is fairly meaningless in assessing the effect of ~~corona-lockdown~~  
299 measures on the concentrations in the central and northern part of the region of interest. ~~This appears to be different~~  
300 ~~for some more southerly areas, e.g. Collivignarelli et al. (2020) identified a 14 day period in February 2020 for~~  
301 ~~Milan, which they could use as pre-lockdown reference to evaluate emission reduction effects, since temperature,~~  
302 ~~relative humidity, precipitation, wind and irradiance was classified to be similar to those in March 2020.~~

303 To further analyse the weather regimes for the first half of 2020 the classification proposed by Hess and  
304 Brezowsky (1977) has been chosen (see also Bissolli and Dittmann (2001)). This classification identifies  
305 predominant synoptic regimes over Central Europe and defines 30 so called 'Großwetterlagen' (GWLs), which  
306 can be isolated by an objective method introduced by James (2007). The underlying data for this analysis were  
307 provided by the German Weather Service. The results of the GWL-classification can be found in ~~supplemented~~  
308 ~~material~~, Table A2

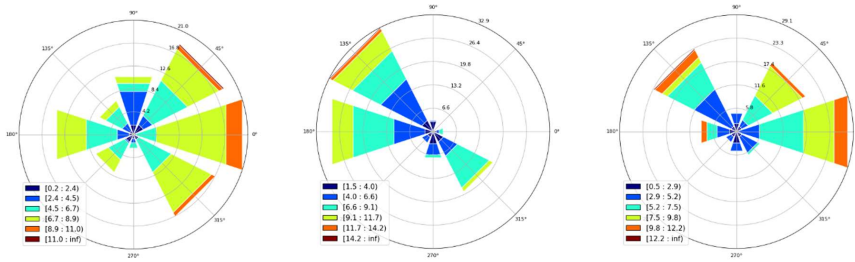
309 **Pre-lockdown period**

310 In February 2020, an unusually wet period occurred due to strong cyclonic activity in Central Europe. Westerly  
311 and North Westerly cyclonic regimes were observed on 76% of the days, whereas high pressure-type regimes  
312 were observed on only 24% of the days Thus, the shortwave downwelling irradiance in February 2020 is one of  
313 the lowest measured at the weather station Wettermast Hamburg (53°31' 09"N and 10°06'10"E)  
314 (<https://wettermast.uni-hamburg.de>) (Brümmer and Schultze, 2015) during the last 25 years (Figure A4), being  
315 representative for north western Europe. The accumulated precipitation for February at this weather station with  
316 an amount of more than 120 mm was exceptionally high compared to the last decades (Figure A4).



319 **Figure 6: 500 hPa geopotential heights (in gpdm) and surface pressure (in hPa) for selected time segments in March**  
 320 **and April 2020 according to the COSMO simulations. The geopotential heights are averaged over 4 days (21.03.-24.03;**  
 321 **6.04.-9.04., 21.04.-24.04. from left to right, respectively). Displayed surface pressure distributions are representative**  
 322 **snap shots within those time segments.**

323



324  
 325 **Figure 7: Wind roses derived from measurements of the weather station Wettermast Hamburg at an altitude of 110 m.**  
 326 **Results for 3 periods covering about 15 days each are shown: 16.03. – 31.03.2020; 1.04.-15.04.2020; 16.04-30.04.2020,**  
 327 **from left to right.**

328

329 **Main lockdown period**

330 For the meteorological characterisation of the main lockdown period between mid of March and end of April we  
 331 rely in addition to the GWL analysis on maps of the 500 hPa geopotential height and the surface pressure  
 332 distribution. The underlying data were extracted from simulations with the COSMO-MERRA system, the same  
 333 meteorological fields; which have been used for the chemistry transport calculations with CMAQ displayed and  
 334 discussed in the following chapters. In [Figure-Fig. 6](#) a subset of those maps for 3 selected time periods is shown;  
 335 the complete set of maps generated can be found in the appendix ([Fig. A5](#)). To characterise and quantify horizontal  
 336 advection, wind roses derived from observations at the Wettermast Hamburg are displayed in [Figure-Fig. 7](#). The  
 337 wind data in each plot cover a time period of about 15 days. Measurements at an altitude of 110 m were chosen  
 338 to better represent a larger area and eliminate parts of the surface influences on the wind.

339 In mid of March, the synoptic regime substantially changed over Europe. ‘High pressure’-type GWLs became  
 340 dominant, i.e. high ridges over Central Europe and high-pressure systems led to a typical atmospheric blocking of  
 341 cyclones. The weather situation shows first a varying blocking in North- and Central Europe followed by a high  
 342 pressure ridge reaching ~~from~~ from the Azores to Scandinavia ([Figure 6](#), left), which changed to a high pressure ridge  
 343 stretching from Iceland into Russia. In northern Germany the wind regime was dominated by a flow with mainly  
 344 easterly components, which were relatively high wind speeds ([Figure-Fig. 7](#), left). In southern Europe the situation,  
 345 which was similar at the beginning of the period to that one in the North, changes starting about on the 23rd of  
 346 March, an isolated trough formed leading to low pressure system activity. For March 28 and 29 dust transport  
 347 from Asia and Northern Africa to the Po Valley was reported ([Collivignarelli et al., 2020](#)).

348 In the first half of April the weather in the north-eastern part of Central Europe was again quite variable, and in  
 349 Southern Europe the cut-off from the northern regime could still be recognized. In the western part of Central  
 350 Europe a ridge has established, which stretched towards the UK. Accordingly, winds in Northern Germany blew

351 predominantly from westerly/north westerly directions. Later on, a ridge over entire Central Europe dominated  
352 the weather in the study domain (Figure 6, middle), only the Eastern Mediterranean was still influenced by a cut-  
353 off trough. In the Po valley, according to measurements around Milan, the weather during the second half of  
354 March to April 10th was dry and very sunny with low to medium wind speeds (Collivignarelli et al., 2020).  
355 Towards the mid of April a high pressure bridge was established reaching from Iceland into Eastern Europe.  
356 In the second half of April a high pressure system established over the British Isles attached to a ridge located  
357 over Central Europe leading to dry and sunny weather all over Europe. This condition was basically stable until  
358 April 25th, when a cyclonic flow took over, leading to more westerly winds over Central Europe, a situation which  
359 lasted until the first days of May. Winds in northern Germany switched over from easterly to more westerly  
360 directions this time (Figure-Fig. 7, right).  
361 Overall, an exceptionally dry period occurred which started in the early lockdown period and continued until the  
362 end of April. The weather was characterized by very low cloud cover and record-breaking large amounts of solar  
363 irradiance (see the record at the Wettermast Hamburg in Fig. A4) and little precipitation. This exceptional weather  
364 period is also discussed by van Heerwaarden et al. (2021), who reported record breaking solar irradiation for the  
365 Netherlands.

#### 366 Lockdown transition

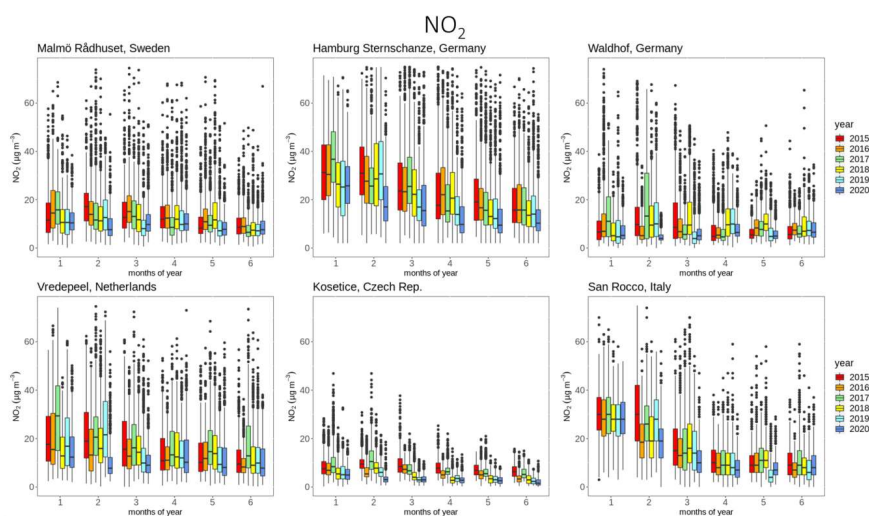
367 In May 2020, atmospheric conditions were very different in Central Europe compared to the previous months. For  
368 instance, Germany was dominated by large amounts of rain in the sSouth, sunny conditions in the wWest and dry  
369 but cloudy conditions in the Eeast and Nnorth. Observed sunshine duration and solar irradiance corresponds  
370 approximately to average climatic conditions. In contrast, large parts of WWestern Europe (Netherlands, Belgium,  
371 West Germany, UK) experienced sunny and dry weather throughout the entire May (van Heerwaarden et al.,  
372 2021). Finally, the large scale conditions in June turned out to favour long-lasting periods with dry and sunny  
373 weather conditions in Nnorthern Germany due to blocking conditions caused by high pressure systems located  
374 over Scandinavia. However, the more southerly regions were rather too wet in a climatological sense.

#### 375 4.2 Concentrations of NO<sub>2</sub>, O<sub>3</sub> and PM<sub>2.5</sub>

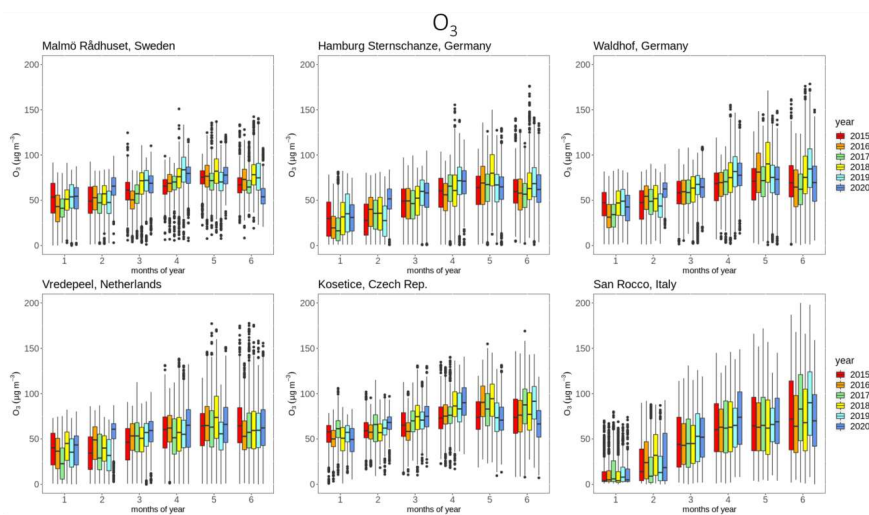
376 The reduced emissions of pollutants during the lockdown periods, ~~which are pronounced in certain sectors,~~ should  
377 lead to changes in ambient concentrations of those substances and related secondary pollutants as ozone. Beside  
378 regional emissions ~~also~~ advected pollutants and the meteorological conditions also determine local and regional  
379 concentrations. To assess changes in air quality and alterations in the behaviour and nature of concentration, time  
380 series observations at selected air quality measurement stations have been examined. The analysed stations have  
381 been selected in a way that they are geographically distributed over the study domain and represent different  
382 emission characteristics. The stations Radhuset in Malmö, Sweden, and Sternschanze in Hamburg, Germany, are  
383 classified as urban background stations, not directly influenced by traffic. ~~In Malmö, the station is located in the  
384 historical part of the town near the town hall, the Hamburg station is placed in a park of a quite lively quarter of  
385 the town. Both urban background stations may be influenced by ship traffic.~~ Waldhof is a rural background station  
386 in northern Germany located about 60 km north of the city of Hannover. Vredepeel is a background station in a  
387 fairly populated part of the Netherlands situated in the triangle between the cities Nijmegen, Eindhoven and Venlo.  
388 The observatory Kosetice in the Czech Republic is located in the Moravian Highlands in an agricultural

Formatiert: Schriftart: Fett

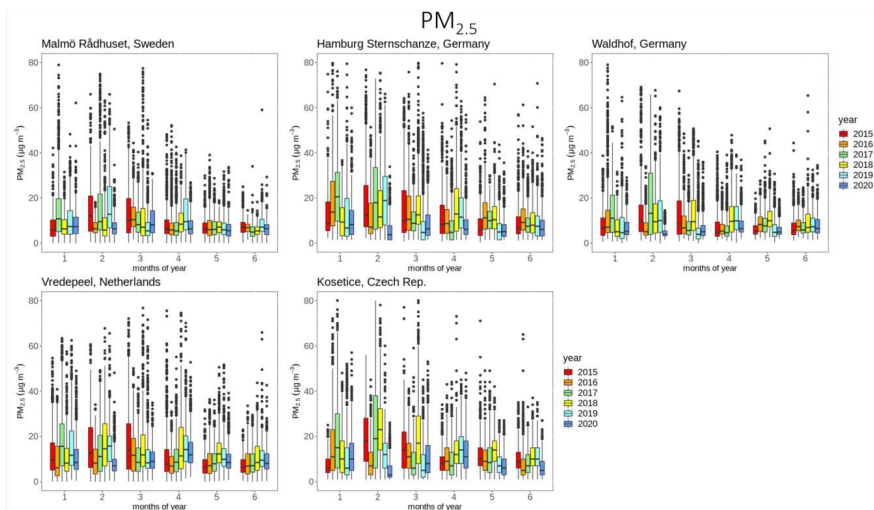
389 countryside about 80 km from south-east of Prague. To represent a region south of the Alps the Italian station San  
 390 Rocco in Po-Valley about 30km east of Parma has been selected. With the exception of Kosetice, having an  
 391 elevation of about 530m, the stations are situated below an altitude of 80m. To allow a comparison of the  
 392 concentration measurements under different meteorological influences, time series of NO<sub>2</sub>, O<sub>3</sub>, and PM<sub>2.5</sub> for the  
 393 years 2015 to 2020 have been examined. However, PM<sub>2.5</sub> was not available at the station San Rocco.  
 394



395



396



397

398 **Fig. 8: Observed monthly concentrations of  $\text{NO}_2$ ,  $\text{O}_3$ , and  $\text{PM}_{2.5}$  at Waldhof (Germany), Vredepeel (The Netherlands),**  
 399 **San Rocco (Italy), Kosetice (Czech Republic), Malmö (Sweden) and Hamburg (Germany). The median is displayed**  
 400 **within the central boxes which span from the 25th percentile to the 75th percentile, called the interquartile range of**  
 401 **the underlying frequency distributions. For  $\text{NO}_2$  and  $\text{PM}_{2.5}$  these distributions are based on hourly measurements at**  
 402 **the different stations and for  $\text{O}_3$  on daily 8 hour maximum values. The whiskers above and below the central boxes**  
 403 **indicate the largest and the smallest value within 1.5 times the interquartile range, respectively. Dots denote values**  
 404 **outside these ranges.  $\text{PM}_{2.5}$  was not available at San Rocco.**

405 The observational results for the selected stations for  $\text{NO}_2$ ,  $\text{O}_3$ , and  $\text{PM}_{2.5}$  are displayed in Fig. 8. For  $\text{NO}_2$ , at all  
 406 stations, with the exception of Waldhof, an obvious trend from higher concentrations in the winter months to  
 407 lower ones in spring in early summer can be seen. At Waldhof this trend is not that clear due to lower values in  
 408 January for most of the years. As it can be expected, in urban (Malmö and Hamburg) or densely populated  
 409 (Vredepeel and San Rocco) regions the  $\text{NO}_2$  concentration are on a higher level. At most stations the  $\text{NO}_2$   
 410 concentrations for March 2020, the month during which in all countries the lockdown measures started, are among  
 411 the lowest ones compared to the previous years. For Hamburg, Vredepeel and Kosetice this also holds for the  
 412 months April to June. An obvious feature, which appears at all stations except San Rocco is, that the February  
 413 concentrations in 2020 are lower compared to the previous years, although no lockdown measures were taken in  
 414 Europe in February. Presumably, meteorological conditions are responsible for these relatively low  $\text{NO}_2$   
 415 concentrations. February 2020 was a month with steady westerly winds and longer periods of intense precipitation  
 416 in Northern Europe. While strong winds cause rapid dilution of pollutants, steady precipitation has a cleaning  
 417 effect due to dissolution of pollutants in cloud and rainwater and subsequent wash-out.

418 For  $\text{O}_3$ , at all stations and for all years the typical trend from low winter concentrations to higher concentrations  
 419 in spring and early summer can be seen. During the lockdown month April the  $\text{O}_3$  concentrations for the years  
 420 2018, 2019, 2020 were higher than in the previous years. During those years the radiation was rather intense in  
 421 April, which favours the photochemical formation of ozone. At the rural stations Waldhof and Kosetice ozone  
 422 concentrations in May and June 2020 were lower than in previous years. At the urban stations in Malmö and  
 423 Hamburg the relative increase in  $\text{O}_3$  concentrations over the 6 month period is lower compared to the more rural  
 424 stations. This can be interpreted as a titration effect of  $\text{O}_3$  by reactions with  $\text{NO}$ , which has significant sources in

**Formatiert:** Schriftart: 9 Pt., Fett, Nicht Kursiv, Schriftfarbe: Automatisch

**Formatiert:** Schriftart: 9 Pt., Fett, Nicht Kursiv, Schriftfarbe: Automatisch

425 urban areas. In general, the observations of O<sub>3</sub> maxima do not provide any indication of significant effects related  
426 to lockdown emission changes in 2020. Possible effects of NO emission drops in March and April 2020 might be  
427 low and masked by meteorological conditions.

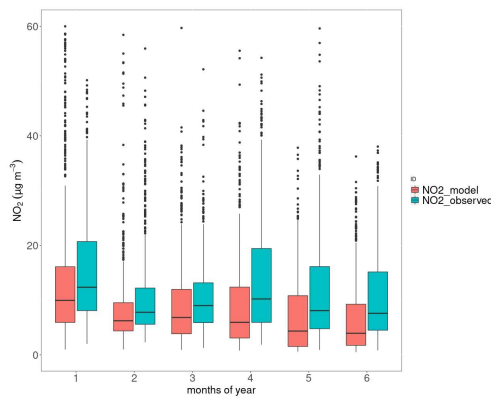
428 PM<sub>2.5</sub> concentrations also show no clear signal that would allow to relate concentrations to lockdown emission  
429 reductions. Slightly higher concentrations and variability can be observed in winter compared to summer at all  
430 stations. This can be related to the fact that very high PM concentrations appear in winter, only, when emissions  
431 are high and atmospheric mixing is suppressed, e.g. during high pressure situations with advection of cold air.  
432 Similar to the NO<sub>2</sub> concentrations, rainy and windy weather in February 2020 leads to low PM<sub>2.5</sub> concentrations  
433 at all stations.

### 434 4.3 Model results at measurement stations

435 In order to judge the quality of the model results, simulated concentrations were compared to observations at  
436 selected stations, including some of those presented above. Fig. 9 exemplarily shows the comparison at Vredepeel.  
437 Table 1 contains statistical values for NO<sub>2</sub> and O<sub>3</sub> at 11 stations and for PM<sub>2.5</sub> at 4 stations in Europe.

438 Modelled NO<sub>2</sub> concentrations are typically lower than the observed values, in particular, the model shows a  
439 stronger downward trend of the concentrations in spring than observed. This pattern is reversed for ozone, where  
440 the modelled 8h max concentrations are typically too high with better agreement in spring compared to winter.  
441 PM<sub>2.5</sub> is underestimated on average, but only at 2 out of 4 stations. Here, the agreement is typically better in winter  
442 compared to spring. As average for all selected stations, the model bias for NO<sub>2</sub> is -17%, for O<sub>3</sub> it is +21% and  
443 for PM<sub>2.5</sub> it is -5%. The temporal correlation (R<sup>2</sup>) based on daily mean values varies between 0.42 and 0.74 for  
444 NO<sub>2</sub>, between 0.07 and 0.75 for O<sub>3</sub> and between 0.21 and 0.62 for PM<sub>2.5</sub>. Details are given in Table 1.

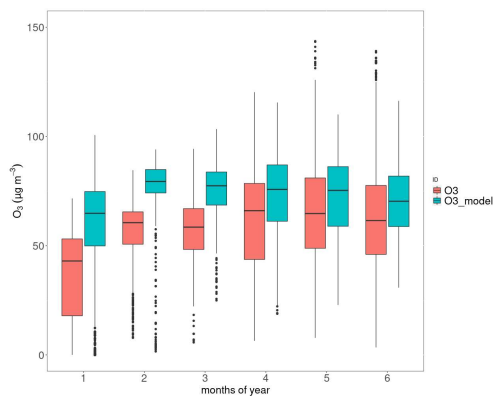
Formatiert: Überschrift 2, Abstand Vor: 12 Pt., Nach:  
12 Pt., Zeilenabstand: einfach



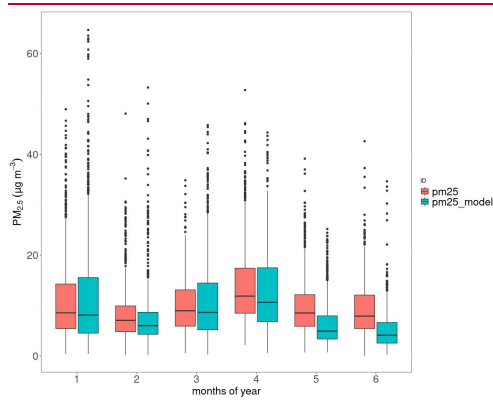
445



446



447



448 **Fig. 9: Comparison between model results (green) and observations (red) at Vredepeel, Netherlands. Top: NO<sub>2</sub>, middle:**  
 449 **O<sub>3</sub>, bottom: PM<sub>2.5</sub>. All concentrations are given in µg/m<sup>3</sup>, box plots show medians, 25% and 75% quartiles and whiskers**  
 450 **representing 1.5 times the interquartile range. Values that fall outside the range of the whiskers are given as dots.**

451

452 **Table 1: Statistical evaluation of a comparison between observations of NO<sub>2</sub> at selected background stations of the EEA**  
 453 **network with CMAQ model results between 1 Jan 2020 and 30 June 2020**

Station	Observed [µg/m <sup>3</sup> ]	Modelled (COV case) [µg/m <sup>3</sup> ]	Bias (model- obs) [µg/m <sup>3</sup> ]	Correlation
<b>NO<sub>2</sub> concentrations 1 Jan 2020 – 30 June 2020</b>				
<u>Risoe, DK</u>	<u>4.7</u>	<u>5.7</u>	<u>1.0</u>	<u>0.46</u>
<u>Waldhof, DE</u>	<u>5.0</u>	<u>3.8</u>	<u>-1.2</u>	<u>0.63</u>
<u>Zingst, DE</u>	<u>4.4</u>	<u>2.9</u>	<u>-1.5</u>	<u>0.63</u>

<u>Neuglobsow, DE</u>	<u>2.9</u>	<u>2.6</u>	<u>-0.3</u>	<u>0.66</u>
<u>Vredepeel, NL</u>	<u>12.4</u>	<u>10.2</u>	<u>-2.2</u>	<u>0.64</u>
<u>De Zilk, NL</u>	<u>11.4</u>	<u>12.8</u>	<u>1.4</u>	<u>0.51</u>
<u>Kosetice, CZ</u>	<u>3.4</u>	<u>3.0</u>	<u>-0.3</u>	<u>0.42</u>
<u>San Rocco, IT</u>	<u>13.5</u>	<u>9.2</u>	<u>-4.3</u>	<u>0.74</u>
<u>Besenzone, IT</u>	<u>15.8</u>	<u>11.9</u>	<u>-3.9</u>	<u>0.71</u>
<u>Casirate d'adda, IT</u>	<u>19.4</u>	<u>15.9</u>	<u>-3.5</u>	<u>0.71</u>
<u>Paray le Fresil, FR</u>	<u>3.1</u>	<u>2.1</u>	<u>-1.0</u>	<u>0.54</u>
<u>O<sub>3</sub> concentrations 1 Jan 2020 – 30 June 2020</u>				
<u>Risoe, DK</u>	<u>71.2</u>	<u>75.7</u>	<u>4.5</u>	<u>0.07</u>
<u>Waldhof, DE</u>	<u>63.6</u>	<u>74.5</u>	<u>10.9</u>	<u>0.25</u>
<u>Zingst, DE</u>	<u>70.6</u>	<u>79.7</u>	<u>9.1</u>	<u>0.23</u>
<u>Neuglobsow, DE</u>	<u>62.8</u>	<u>74.8</u>	<u>12.0</u>	<u>0.16</u>
<u>Vredepeel, NL</u>	<u>56.8</u>	<u>70.5</u>	<u>13.7</u>	<u>0.55</u>
<u>De Zilk, NL</u>	<u>63.1</u>	<u>70.6</u>	<u>7.5</u>	<u>0.34</u>
<u>Kosetice, CZ</u>	<u>70.0</u>	<u>78.6</u>	<u>8.6</u>	<u>0.21</u>
<u>San Rocco, IT</u>	<u>54.7</u>	<u>73.4</u>	<u>18.7</u>	<u>0.68</u>
<u>Besenzone, IT</u>	<u>49.5</u>	<u>69.3</u>	<u>19.8</u>	<u>0.59</u>
<u>Casirate d'adda, IT</u>	<u>56.3</u>	<u>74.0</u>	<u>17.7</u>	<u>0.75</u>
<u>Paray le Fresil, FR</u>	<u>58.6</u>	<u>77.2</u>	<u>18.6</u>	<u>0.43</u>
<u>PM<sub>2.5</sub> concentrations 1 Jan 2020 – 30 June 2020</u>				
<u>Waldhof, DE</u>	<u>6.8</u>	<u>7.3</u>	<u>0.5</u>	<u>0.21</u>
<u>Vredepeel, NL</u>	<u>10.6</u>	<u>9.2</u>	<u>-1.4</u>	<u>0.57</u>
<u>De Zilk, NL</u>	<u>6.8</u>	<u>7.8</u>	<u>1.0</u>	<u>0.44</u>

Kosetice, CZ	9.3	7.8	-1.5	0.62
--------------	-----	-----	------	------

454

455 **5 COVID-19 lockdown effects**

456 Effects of the lockdown measures on emissions were discussed in section 3. Now, CMAQ model results are  
 457 evaluated for the COV and the noCOV case during the lockdown phase. Meteorological impacts are discussed  
 458 through comparisons of CMAQ model results that were derived with meteorological data for the years 2016 and  
 459 2018.

460 **5.1 CMAQ results for Central Europe**

461 Differences between the CMAQ results for 2020 for the COV and the noCOV case reveal the impact of the  
 462 lockdown emission reductions on air pollutant concentrations. The magnitude of the concentration changes varies  
 463 considerably in time and space. Here, we focus our evaluation on the period with the highest emissions reductions  
 464 between 16 and 31 March 2020. During this time the most widely spread and temporally stable emission  
 465 reductions took place in Europe. Differences among weekdays and weekends and, to a limited extent, also among  
 466 different weather situations are averaged out by investigating a half-month-period. However, changing effects  
 467 over time are also discussed.

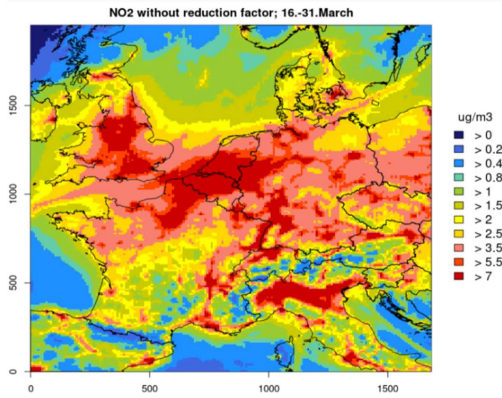
468 **NO<sub>2</sub> concentrations**

469 Fig. [ure 109](#) shows maps of the modelled average NO<sub>2</sub> concentrations in Central Europe between 16 and 31 March  
 470 for the case without lockdown measures (noCOV) together with the absolute and relative concentration reductions  
 471 caused by the lockdown. The NO<sub>2</sub> concentrations for the noCOV case in central Europe show the typical pattern  
 472 with highest concentrations in densely populated areas like England, Belgium, The Netherlands and western  
 473 Germany as well as northern Italy (Fig [109a](#)). Average concentrations range between 5 and 10 µg/m<sup>3</sup>. Reductions  
 474 in NO<sub>2</sub> concentrations caused by the lockdown are highest in the same regions, also reaching several µg/m<sup>3</sup>.  
 475 Relative reductions are highest in France, Belgium, Italy, and Austria, reaching more than 40% on average.  
 476 Germany, [T](#)he Netherlands, UK, southern Sweden and the Czech Republic show lower reductions between 15%  
 477 and 30%. In the following weeks, NO<sub>2</sub> concentrations stayed more or less on the same level in most parts of  
 478 Europe, but the lockdown effects decreased slightly as it could be expected from the emission changes. Overall,  
 479 relative concentration reductions were most significant in England, France, Belgium and Italy, as it was seen for  
 480 the second half of March. Maps for relative reductions due to the lockdown for six half-month periods between 1  
 481 March 2020 and 31 May 2020 are given in the appendix (Fig A6).

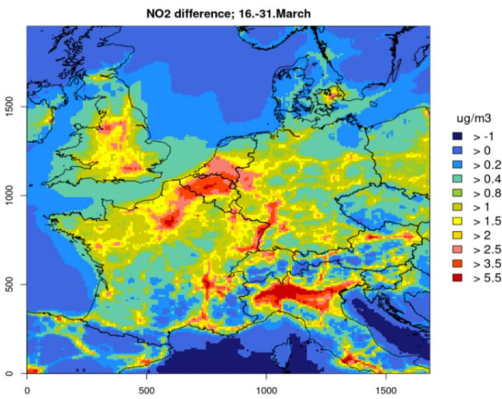
Formatiert: Schriftart: (Standard) Arial, 11 Pt.

Formatiert: Links, Zeilenabstand: Mehrere 1,15 ze

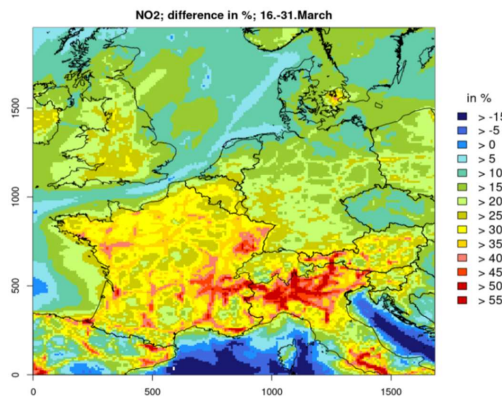
482



483



484



485 Figure 109: CMAQ results for NO<sub>2</sub> concentrations in Central Europe between 16 and 31 March 2020. Top:  
486 Concentrations without lockdown measures (noCOV run). Middle: Absolute concentration reductions due to lockdown  
487 measures (noCOV – COV run). Bottom: Relative concentration reductions due to lockdown measures (noCOV – COV  
488 run); positive values for absolute and relative differences denote high reductions.

489 **O<sub>3</sub> concentrations**

490 It can be expected that reduced NO<sub>x</sub> emissions are also reflected in modified O<sub>3</sub> concentrations with lower values  
491 in all regions that are NO<sub>x</sub>-limited. However, for the second half of March increased O<sub>3</sub> concentrations between  
492 1 and 8 µg/m<sup>3</sup> were modelled in the COV case for northern Central Europe and the Po valley (see Fig. 110).  
493 Because these are the regions with the highest NO<sub>x</sub> emissions in Europe, they were most likely VOC-limited  
494 during this first lockdown period and O<sub>3</sub> titration with NO was reduced when NO<sub>x</sub> emissions were reduced. Most  
495 of the southern parts of the modelling domain exhibited a decrease in ozone of 1-2 µg/m<sup>3</sup> on average caused by  
496 the lockdown and the reduced NO<sub>x</sub> emissions. In the following weeks, areas with increased ozone turned smaller  
497 week by week and were limited to large cities and the most densely populated areas, see Fig 121 for the first half  
498 of April and the first half of May. Most regions in Europe turned into NO<sub>x</sub>-limited areas in spring 2020, resulting  
499 in lower ozone concentrations of 1-2 µg/m<sup>3</sup> (about 2-4% change) caused by the emission changes during the  
500 lockdown (see Fig. A7 in the supplement).

Formatiert: Tiefgestellt

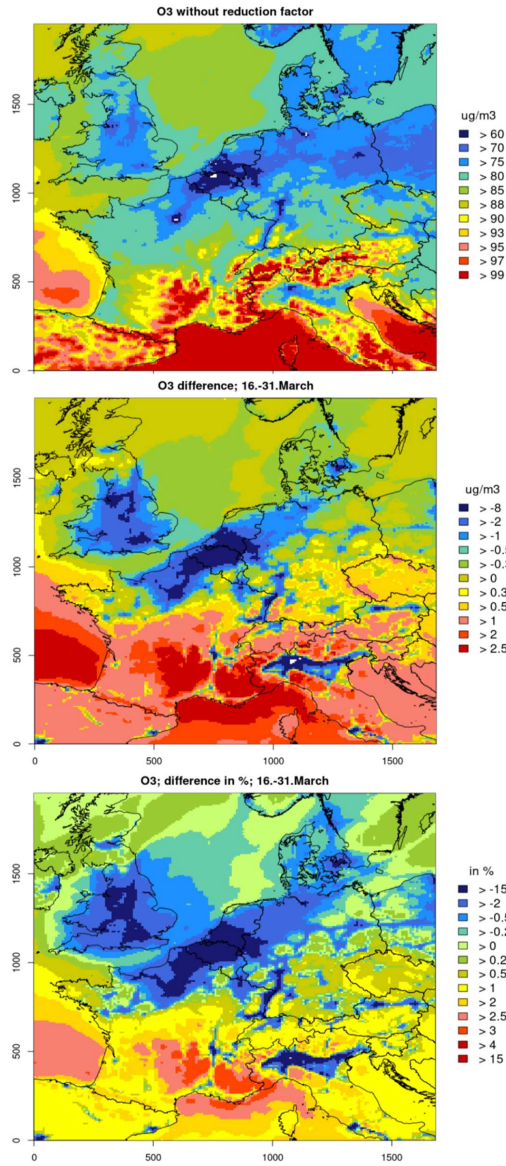
Formatiert: Tiefgestellt

Formatiert: Tiefgestellt

Formatiert: Tiefgestellt

Formatiert: Tiefgestellt

Formatiert: Tiefgestellt



501

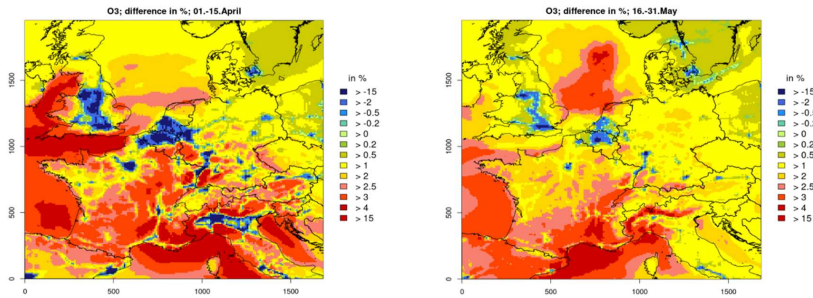
502

503

504

505 **Fig. 110:** CMAQ results for O<sub>3</sub> concentrations in Central Europe between 16 and 31 March 2020. Top: Concentrations  
 506 without lockdown measures (noCOV run). Middle: Absolute concentration reductions due to lockdown measures  
 507 (noCOV – COV run); positive values denote high reductions. Bottom: Relative concentration reductions due to  
 508 lockdown measures (noCOV – COV run); positive values denote reductions, negative values denote increases.

509



510

511 **Fig. 124:** CMAQ results for changes in O<sub>3</sub> concentrations due to lockdown measures in Central Europe between 1 and  
512 15 April 2020 (left) and 16-31 May 2020 (right). Positive values denote concentration reductions, negative values denote  
513 concentration increases.

#### 514 **PM<sub>2.5</sub> concentrations**

515 Simulated PM<sub>2.5</sub> concentrations in the second half of March 2020 for the noCOV case show relatively high  
516 concentrations between 12 and 15 µg/m<sup>3</sup> in large parts of Central Europe and the Po valley while the UK, Denmark  
517 and Northern Germany exhibited concentrations below 10 µg/m<sup>3</sup> (see Fig. 132, top). The lockdown emission  
518 reductions lead to concentration reductions between 1 and 3 µg/m<sup>3</sup> in those regions with higher concentrations  
519 and values below 1 µg/m<sup>3</sup> in the north western part of the domain. Relative concentration decreases were most  
520 significant in France and Northern Italy with values up to 20% while in the rest of the domain 6-10% lower PM<sub>2.5</sub>  
521 was simulated. In the following weeks, PM<sub>2.5</sub> concentrations were typically reduced by 10-20% because of the  
522 lockdown measures in most parts of Central Europe. Somewhat lower values were found in the Northern and  
523 southern parts of the domain. The reduction in PM<sub>2.5</sub>- concentrations decreased to 6-12% in the second half of  
524 May (see Fig. A8 in the supplement).

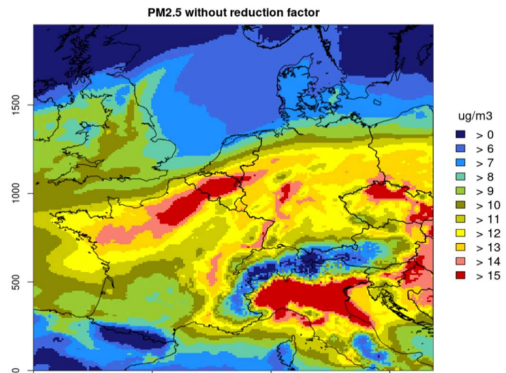
525 An investigation of the chemical components of the modelled PM<sub>2.5</sub> concentrations for the noCOV case reveals  
526 that about 2/3 consists of the inorganic components nitrate (NO<sub>3</sub><sup>-</sup>), sulphate (SO<sub>4</sub><sup>2-</sup>) and ammonium (NH<sub>4</sub><sup>+</sup>). The  
527 lockdown measures caused large reductions in NO<sub>x</sub> emissions. Consequently, nitrate was reduced by more than  
528 24% in large parts of France and northern Italy between mid of March and end of April, see Fig. A9 in the  
529 appendix. The reduction was usually somewhat lower in other parts of the domain. Particulate nitrate is mostly  
530 bound to ammonium, however, the model results show a lower relative reduction of the ammonium concentrations  
531 compared to nitrate. It is only in the order of 8-20% at maximum (Fig. A10). This is because ammonium is  
532 preferably bound to sulphate in atmospheric aerosols and sulphate concentrations even increased by a few percent  
533 as a consequence of the lockdown measures (Fig. A11). This can be explained by the large reduction in the  
534 formation of particulate nitrate in the COV case. Less nitrate means less ammonium which is then available as  
535 gaseous ammonia. This may lead to the formation of additional ammonium sulphate in areas where gaseous  
536 sulphuric acid is available.

Formatiert: Tiefgestellt

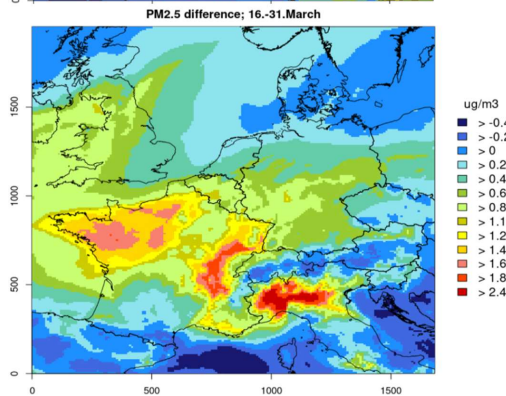
Formatiert: Hochgestellt

Formatiert: Tiefgestellt

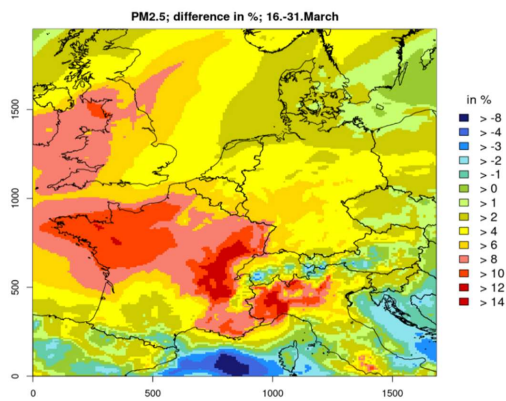
537



538



539



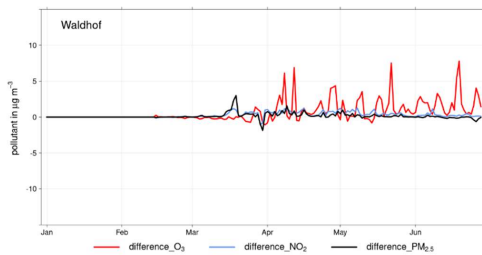
540

541 **Fig. 132:** CMAQ results for PM2.5 concentrations in Central Europe between 16 and 31 March 2020. Top:  
 542 Concentrations without lockdown measures (noCOV run).Middle: Absolute concentration reductions due to lockdown  
 543 measures (noCOV – COV run); positive values denote reductions. Bottom: Relative concentration reductions due to  
 544 lockdown measures (noCOV – COV run); positive values denote reductions.

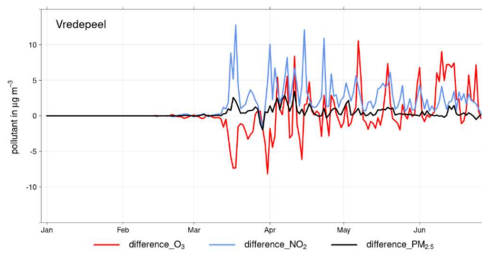


545 **Temporal development of concentration changes**

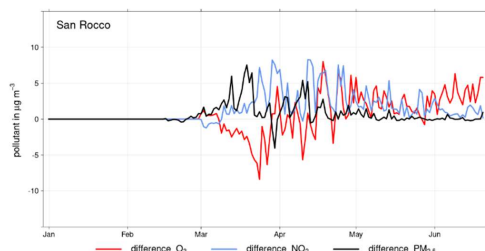
546 The detailed temporal development of the effect of lockdown emission reductions on atmospheric concentrations  
547 of NO<sub>2</sub>, O<sub>3</sub> and PM<sub>2.5</sub> is followed at selected measurement stations. Figure 143 shows the modelled differences  
548 between the noCOV and the COV model runs at Waldhof, Vredepeel, and San Rocco. Lockdown emission  
549 reductions lead to reduced concentrations of NO<sub>2</sub> and PM<sub>2.5</sub> at all stations, however, the amount varies  
550 considerably in time and by station. At Waldhof, only very small changes are observed/simulated. At Vredepeel,  
551 NO<sub>2</sub> is significantly reduced (by more than 10 µg/m<sup>3</sup> on individual days) PM<sub>2.5</sub> shows only small reductions. At  
552 San Rocco, both, NO<sub>2</sub> and PM<sub>2.5</sub> are reduced by several µg/m<sup>3</sup> until the end of April. In May and June, lockdown  
553 effects on the concentrations get much smaller, also at Vredepeel and San Rocco.  
554 O<sub>3</sub> shows higher values despite the emission reductions until mid of April at Vredepeel and San Rocco. This is  
555 because these stations are in VOC-limited areas at that time, where NOx emission reductions lead to decreased  
556 O<sub>3</sub> titration. This pattern changes towards end of April and in the following O<sub>3</sub> is decreased on most of the days  
557 at all stations as a consequence of lower NOx emissions. This effect remains variable at Vredepeel, a station close  
558 to the region with highest NOx emissions in Europe. At Waldhof, O<sub>3</sub> reductions are observed between beginning  
559 of April and end of June. On average between 16 March and 30 June, O<sub>3</sub> is only decreased by 0.6 µg/m<sup>3</sup> (< 1%)  
560 at Vredepeel. At Waldhof and San Rocco, the reductions are 1.2 µg/m<sup>3</sup> (1.6%) and 1.5 µg/m<sup>3</sup> (1.9%), respectively.



561



562



563

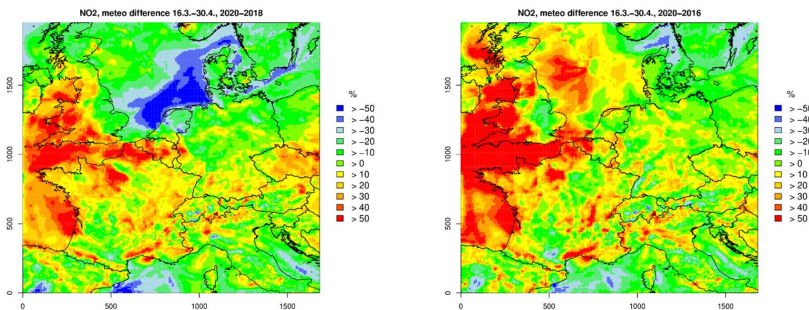
564 **Fig. 143:** Temporal development of the differences in the simulated concentrations of O<sub>3</sub> (red), NO<sub>2</sub> (blue) and PM<sub>2.5</sub>  
 565 (black) in Waldhof (top), Vredepeel (middle) and San Rocco (bottom) between 1 January and 30 June 2020.

566 **5.2 Impact of meteorological conditions**

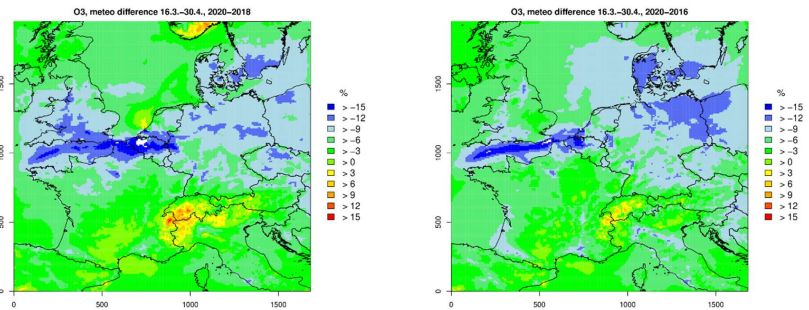
567 For investigating the effects of the exceptional meteorological situation on the concentration reductions in March  
 568 and April 2020, additional CMAQ model simulations were performed. Meteorological data simulated with  
 569 COSMO-CLM for the first six months in 2016 and 2018 was used as input data, together with the 2020 emissions  
 570 for both; the COV and the noCOV case. Biogenic emissions were also kept the same for the 2016 and 2018 runs  
 571 in order to investigate effects of meteorological conditions; only. These additional years were selected to cover a  
 572 span of weather situations during the lockdown phase. The selected years were different, but represent not in any  
 573 sense an extreme situation. They were chosen from the time span 2015 to 2019, since for these years model data  
 574 generated using the same advanced model settings (model version and reanalysis data) is available. The results  
 575 show the concentration and the changes caused by the lockdown measures as they would have happened under  
 576 different meteorological conditions.

577 Fig. 154, top, shows the NO<sub>2</sub> concentration changes for 2020 relative to 2018 and 2016 caused by meteorological  
 578 conditions, only, for the period between 16 March and 30 April. No emission changes because of the lockdown  
 579 were assumed for this investigation. Meteorological conditions in 2020 caused between 20% and more than 30%  
 580 lower NO<sub>2</sub> concentrations in large areas of the nNorth eEastern model domain (The Netherlands, nNorthern  
 581 Germany, Denmark and sSouthern Sweden) compared to 2018, even without any lockdown measures. On the  
 582 other hand, in western UK, Belgium, Nnothern France, and the Czech Republic, meteorological conditions lead  
 583 to 20% to more than 30% higher NO<sub>2</sub> concentrations. The picture is similar when compared to 2016, in particular  
 584 in the western part of the model domain, but the area with lower NO<sub>2</sub> concentrations in 2020 compared to 2016  
 585 does not include the North Sea and Denmark.

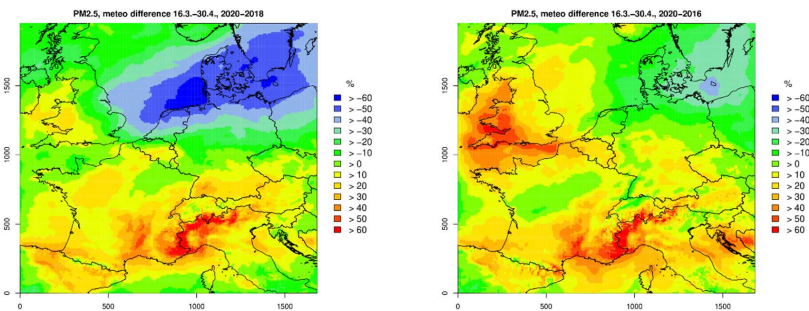
586



587



588



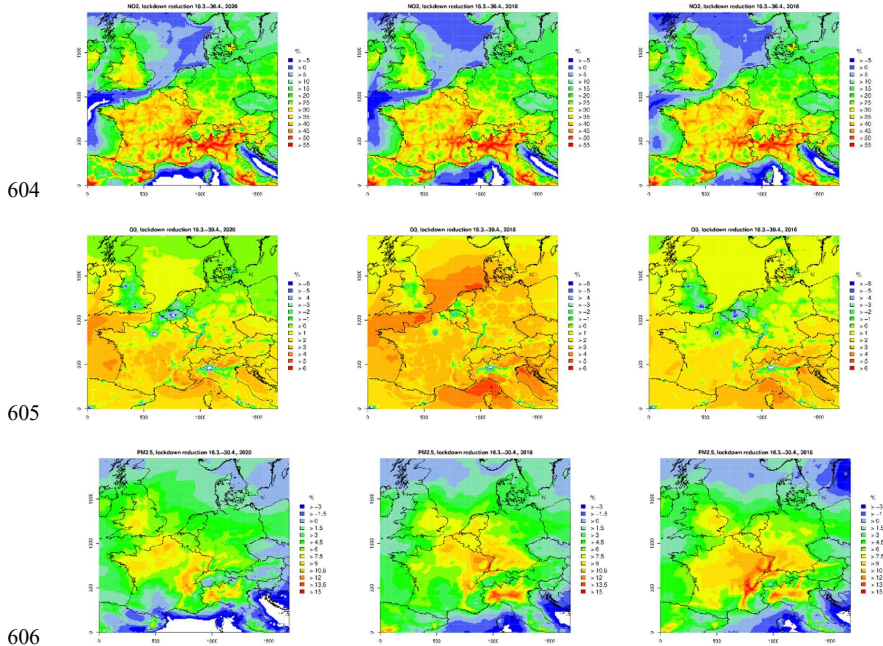
589 **Fig. 154:** Relative concentration changes due to meteorological conditions in Central Europe between 16 March and 30  
590 April simulated with CMAQ for NO<sub>2</sub> (top), O<sub>3</sub> (middle) and PM<sub>2.5</sub> (bottom): The changes are represented as relative  
591 numbers for 2020 compared to 2018 (left) and 2016 (right). Positive values denote higher concentrations in 2020 relative  
592 to the previous year. Be aware of the different scales for each pollutant.

593 Average ozone concentrations between 16 March and 30 April 2020 were relatively low in almost entire Central  
594 Europe when compared to a situation with meteorological conditions as in 2018 and 2016 (see Fig. 152, middle).  
595 Differences are in the order of 10-15% in the northern part of the model domain and between 2 and 6-% in the  
596 southern part. Only in few spots in **n**orthern Italy and **S**outhern Switzerland, the meteorological situation in  
597 2020 favoured ozone formation compared to 2016 and 2018.

598 The picture is more mixed for PM<sub>2.5</sub> with considerably lower concentrations in 2020 compared to 2016 and 2018,  
599 particularly in **N**orthern Germany and Poland, i.e. in the north eastern part of the domain (Fig. 15, bottom).

600 Relative differences reach more than 50% between 2020 and 2018 in the German Bight. Compared to 2018, PM<sub>2.5</sub>

601 concentrations were also low in the western UK in 2020. In almost entire France and in Northern Italy, PM<sub>2.5</sub>  
 602 concentrations were relatively high in 2020 compared to 2016 and 2018, differences again reach more than 50%  
 603 but with opposite sign.



607 **Fig. 165:** Relative concentration reductions due to lockdown measures (noCOV – COV run) in Central Europe between  
 608 16 March and 30 April simulated with CMAQ for NO<sub>2</sub> (top), O<sub>3</sub> (middle) and PM<sub>2.5</sub> (bottom) and three different  
 609 meteorological input data sets. Left: 2020, Middle: 2018, Right: 2016. Positive values denote concentration reductions  
 610 caused by the lockdown emission changes. Be aware of the different scales for each pollutant.

611 The meteorological situation also affects the concentration changes caused by the lockdown, but this differs  
 612 considerably among the pollutants. Fig 165 shows the lockdown emission reduction effects on the average  
 613 concentrations for the main lockdown period from 16 March to 30 April. In most parts of Central Europe the  
 614 variation for NO<sub>2</sub> is rather small (plus/minus approx. 5%). For ozone, on the other hand, effects of the lockdown  
 615 are quite different among the three selected meteorological years. For 2020 meteorological conditions, relatively  
 616 large areas in Northern Central Europe show a slight increase in ozone (green and blue areas in Fig. 165, middle  
 617 row). These areas would have been smaller with 2016 meteorological conditions and limited to the most densely  
 618 populated areas for 2018 meteorological conditions. Lockdown effects on PM<sub>2.5</sub> would have been more significant  
 619 under meteorological conditions of the years 2016 and 2018 in almost the entire model domain (Fig. 165, bottom  
 620 row). Particularly in Northern Italy and South Eastern France, changes in PM<sub>2.5</sub> caused by the lockdown could  
 621 be more than 10%, a value that was rarely reached during the real lockdown in 2020.

622 **6 Discussion**

623 **6.1 Time series at selected stations**

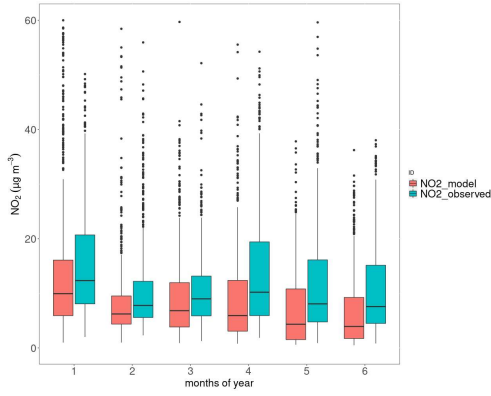
624 Observations of NO<sub>2</sub> and PM<sub>2.5</sub> concentrations in Central Europe in the first six months of 2020 showed low  
625 concentrations in March and April when compared to previous years. According to CMAQ model simulations  
626 that consider lockdown emission reductions as well as emissions that could be expected for 2020, the lockdown  
627 effects are strongest for NO<sub>2</sub> with average concentration reductions up to 40% between mid of March and mid of  
628 April. PM<sub>2.5</sub> shows reduction up to 20% while the effect on O<sub>3</sub> is much lower (up to 4% reduction). O<sub>3</sub>  
629 concentrations might even increase in large parts of northern Europe in March.

630 In order to quantify the quality of these model estimates, the simulated concentrations were compared to  
631 observations at selected stations (including those presented in section 4 and 5). Figure 16 exemplarily shows the  
632 comparison at Vredepeel, Table 1 contains statistical values for NO<sub>2</sub> and O<sub>3</sub> at 11 stations and for PM<sub>2.5</sub> at 4  
633 stations in Europe.

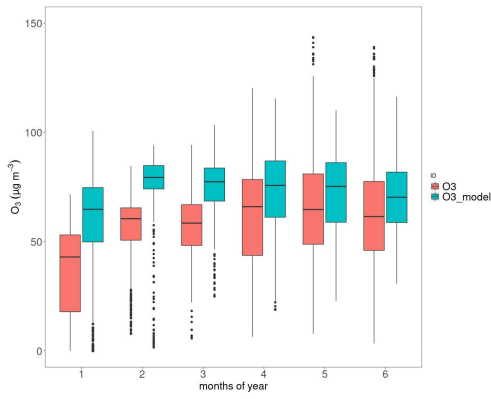
634 Modelled NO<sub>2</sub> concentrations are typically lower than the observed values, in particular, the model shows a  
635 stronger downward trend of the concentrations in spring than observed. This pattern is reversed for ozone, where  
636 the modelled 8h max concentrations are typically too high with better agreement in spring compared to winter.  
637 PM<sub>2.5</sub> is underestimated on average, but only at 2 out of 4 stations. Here, the agreement is typically better in winter  
638 compared to spring. As average for all selected stations, the model bias for NO<sub>2</sub> is -17%, for O<sub>3</sub> it is +21% and  
639 for PM<sub>2.5</sub> it is -5%. The temporal correlation (R<sup>2</sup>) based on daily mean values varies between 0.42 and 0.74 for  
640 NO<sub>2</sub>, between 0.07 and 0.75 for O<sub>3</sub> and between 0.21 and 0.62 for PM<sub>2.5</sub>. Details are given in Table 1.

641 The model is able to reproduce observed concentration levels and their spatiotemporal variation. The agreement  
642 between modelled and observed concentrations is in a range that is typical for regional CTMs (see e.g. Solazzo  
643 et al. (2012)). The deviations from the observed values can be interpreted as relative uncertainties in the modelled  
644 lockdown effects. During the lockdown between March and June, deviations between modelled and observed  
645 concentrations are often higher than the changes caused by the lockdown. Therefore, the results cannot be used to  
646 judge how accurate the estimated emission reductions are.

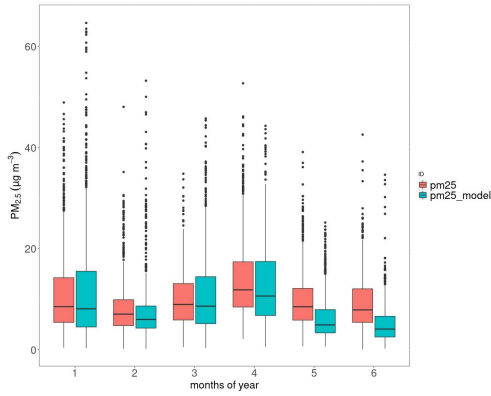
647 Based on the 6 months of simulation, the average concentrations reductions at the 11 selected stations are 14%  
648 (7%–26%) for NO<sub>2</sub>, 0.4% for O<sub>3</sub> (-1.3% to +1.7%) and 2.3% for PM<sub>2.5</sub> (-0.1% to 4.0%). While half year average  
649 NO<sub>2</sub> concentrations in highly polluted areas decreased between 15% (Vredepeel, The Netherlands) and 25%  
650 (Besenzone and Casirate d'adda, Po Valley, Italy), NO<sub>2</sub> reductions are much smaller (7–15%) in rural areas.  
651 Average O<sub>3</sub> concentrations increased slightly (1%) close to cities and decreased in rural areas (up to 2%). For  
652 PM<sub>2.5</sub>, concentration changes at the four measurement stations were mostly between 2 and 4%. Under the  
653 assumption that emission reductions were much lower in the second half of 2020, the lockdown emission  
654 reductions exhibit only very small effects on annual average pollutant concentrations, especially for secondary  
655 pollutants. Concentration reductions at the measurement stations for the main lockdown period (16 March–30  
656 April) are also given in Table 1.



657



658



659

660 **Fig. 16: Comparison between model results (green) and observations (red) at Vredepeel, Netherlands. Top: NO<sub>2</sub>,**  
 661 **middle: O<sub>3</sub>, bottom: PM<sub>2.5</sub>. All concentrations are given in µg/m<sup>3</sup>, box plots show medians, 25% and 75% quartiles and**  
 662 **whiskers representing 1.5 times the interquartile range. Values that fall outside the range of the whiskers are given as**  
 663 **dots.**

664

665  
666

**Table 1: Statistical evaluation of a comparison between observations of NO<sub>2</sub> at selected background stations of the EEA network with CMAQ model results between 1 Jan 2020 and 30 June 2020**

NO <sub>2</sub> concentrations 1 Jan 2020—30 June 2020					
Station	Observed [µg/m <sup>3</sup> ]	Modelled (COV case) [µg/m <sup>3</sup> ]	Bias (model- obs) [µg/m <sup>3</sup> ]	Correlation	Lockdown effect COV <sub>noCOV</sub> (16.3.–30.4.) [µg/m <sup>3</sup> ]
Risoe, DK	4.7	5.7	1.0	0.46	-3.0
Waldhof, DE	5.0	3.8	-1.2	0.63	-0.6
Zingst, DE	4.4	2.9	-1.5	0.63	-0.4
Neuglobsow, DE	2.9	2.6	-0.3	0.66	-0.5
Vredepeel, NL	12.4	10.2	-2.2	0.64	-3.7
De Zilk, NL	11.4	12.8	1.4	0.51	-3.7
Kosetice, CZ	3.4	3.0	-0.3	0.42	-0.6
San Rocco, IT	13.5	9.2	-4.3	0.74	-3.7
Besenzone, IT	15.8	11.9	-3.9	0.71	-7.3
Casirate d'adda, IT	19.4	15.9	-3.5	0.71	-10.5
Paray-le-Fresil, FR	3.1	2.1	-1.0	0.54	-0.9
O <sub>3</sub> concentrations 1 Jan 2020—30 June 2020					
Risoe, DK	71.2	75.7	4.5	0.07	0.5
Waldhof, DE	63.6	74.5	10.9	0.25	-0.7
Zingst, DE	70.6	79.7	9.1	0.23	-0.5
Neuglobsow, DE	62.8	74.8	12.0	0.16	-0.6
Vredepeel, NL	56.8	70.5	13.7	0.55	-0.3
De Zilk, NL	63.1	70.6	7.5	0.34	0.0
Kosetice, CZ	70.0	78.6	8.6	0.21	-1.0

Formatiert: Englisch (Vereinigtes Königreich)

Formatiert: Englisch (Vereinigtes Königreich)

Formatiert: Englisch (Vereinigtes Königreich)

Formatiert: Englisch (Vereinigtes Königreich)

San Rocco, IT	54.7	73.4	18.7	0.68	-0.9
Besenzone, IT	49.5	69.3	19.8	0.59	0.7
Casirate d'adda, IT	56.3	74.0	17.7	0.75	1.0
Paray-le-Fresnil, FR	58.6	77.2	18.6	0.43	-1.3
PM <sub>2.5</sub> concentrations 1 Jan 2020—30 June 2020					
Waldhof, DE	6.8	7.3	0.5	0.21	-0.1
Vredepeel, NL	10.6	9.2	-1.4	0.57	-0.4
De Zilk, NL	6.8	7.8	1.0	0.44	-0.2
Kosetice, CZ	9.3	7.8	-1.5	0.62	0.0

667

#### 668 6.12 Emission estimates

669 Emissions for 2020 were estimated based on data for 2016 and extrapolation factors that resemble the temporal  
670 development of total sectoral emissions during 3 years before 2016. This method leads to emission corrections  
671 that are typically on the order of 10% but may be up to 40%. This method bears some uncertainties, however, in  
672 countries that have a high share in the total emissions in Central Europe, emission trends were rather stable during  
673 the last 20 years. Good agreement between observed and modelled concentrations during the weeks before the  
674 lockdown gives confidence in the method.

675 Estimates for lockdown emission reductions also include several sources of uncertainty. Reduction of NO<sub>x</sub>  
676 emissions from traffic have the largest share in the emission reductions. In this approach, the LAFs applied are  
677 based on google mobility data that resembles all traffic activities, regardless of their real emissions. I.e. no  
678 distinction between trucks and small private cars is made and it seems likely that traffic related to transporting  
679 goods was less reduced than private and commuter traffic. Therefore, emission reductions in traffic might be  
680 overestimated. On the other hand, possible emission increases for residential heating that are related to more  
681 people working from home were ~~considered to be small and neglected here~~ **not considered at all**. Small changes in  
682 other sectors like off-road machinery that might have taken place weren't considered, either.

683 The cubic spline interpolation, applied to derive daily LAFs from monthly statistical data, enables to represent the  
684 mean of each month correctly while giving an assumption on the daily values with a rather smooth curve. This  
685 assumption does not necessarily represent the real daily conditions as extrema in the interpolation always occur  
686 at the start or in the middle of the month, which might not be the case in reality. However, it is an improvement  
687 compared to using monthly averages for each day of the month, as in this case, extreme jumps can occur at the  
688 transition to the next month that author's assume to be more unrealistic. In addition it might resemble the rapid  
689 emission reductions mid of March better than a monthly value.

Formatiert: Tiefgestellt



690 Similar approaches to calculate lockdown adjustment factors were followed by Doumbia et al. (2021) and Guevara  
691 et al. (2021). Both estimate that decreases in NO<sub>x</sub> emissions in Central Europe taking all sectors together were  
692 around 30% in April 2020, which is in very good agreement with the numbers that were derived in this study.  
693 This Doumbia et al. (2021) study focuses on Europe and calculates LAFs for each country in a detailed way based  
694 on the same data source for each sector. Doumbia et al. (2021) use information from other sources than here (e.g.  
695 for aviation, shipping and industry) which are partly less well resolved in time, however, they provide adjustment  
696 factors for the entire world. Also emissions from residential areas were treated differently. While Doumbia et al.  
697 (2021) see an emission increase, they remained unchanged in this study. The reasoning behind this is that the  
698 heating demand is most likely not significantly modified when more people stay at home compared to the case  
699 when they go to work. This assumption is in agreement with earlier estimates by Le Quéré et al. (2020) who  
700 calculated only small emission increases in the sector Residential. Compared to Guevara et al. (2021), the time  
701 period considered in this study is longer and reaches till the end of June 2020.  
702 The modelled reductions in NO<sub>2</sub> concentrations close to ground which are 30–40% on average during the second  
703 half of March are close to what was estimated from satellite observations. Bauwens et al. (2020) report columnar  
704 NO<sub>2</sub> reductions of approx. 20% around Hamburg, Frankfurt and Brussels, 28% for the area around Paris and 33–  
705 38% for Northern Italy. Such values are in quite good agreement with the modelled values in this study.

Formatiert: Tiefgestellt

Formatiert: Schriftart: (Standard) Times New Roman,  
Schriftfarbe: Automatisch

Formatiert: Schriftart: (Standard) Times New Roman,  
Schriftfarbe: Automatisch

Formatiert: Schriftart: (Standard) Times New Roman,  
Schriftfarbe: Automatisch

### 706 6.3 Impact of meteorological conditions on lockdown effects

707 Meteorological conditions play a major role for concentrations of air pollutants. Not only emissions, but also  
708 atmospheric transport and chemical transformation, as well as wet and dry deposition influence atmospheric  
709 concentrations of NO<sub>2</sub>, O<sub>3</sub> and PM<sub>2.5</sub>. To further assess the influence of meteorological conditions on  
710 concentrations of pollutants over Europe, CMAQ was run using emission data for 2020 (noCOV case) but  
711 combined with meteorological input data for two different years, namely 2016 and 2018. These years were  
712 selected, because they represent significantly different meteorological conditions. In the following, the differences  
713 to the year 2020 for the days between 16 March and 30 April, the period that is further investigated, are briefly  
714 summarized. In the supplement (Fig. A9–A11) relevant plots showing differences for the meteorological  
715 parameters 500 hPa geopotential height, total precipitation and global solar radiation can be found. The results are  
716 based on the COSMO-CLM simulations for the respective years. It should be noted that the simulations for 2016  
717 and 2018 do not resemble the real situation during these years, because all emissions and chemical boundary  
718 conditions were for 2020.

### 719 Meteorological differences 2020 versus 2016 and 2018

720 In 2020 the geopotential height at 500 hPa over the British Isles and the North Sea was significantly higher  
721 compared to that in 2016, especially from 1 April onward. This resulted in a constellation, which favours blocking  
722 in 2020. Near surface high pressure systems were amplified and more persistent and weak wind conditions and a  
723 more continental flow dominate. In 2016 stronger winds of Atlantic origin occasionally were observed. In 2020  
724 precipitation was considerably lower compared to 2016. In most parts of the study region solar radiation was  
725 clearly higher in 2020, especially over Central Europe up to the British Isles.

726 Much of what has been said concerning the blocking condition in 2020 holds as well when compared to 2018.  
727 The year 2020 also was much drier and incoming solar radiation was more intense. In 2018 winds had a more

Formatiert: Überschrift 2, Abstand Vor: 12 Pt., Nach:  
12 Pt., Zeilenabstand: einfach

easterly to south-easterly component. The spatial and temporal distribution and the absolute values of the meteorological parameters were slightly different in 2018 compared to 2016 (see Fig. A9–A11), so this year became an additional choice for the evaluation of meteorological influences.

### 6.3 CTM results

Chemistry transport model simulations are always connected with uncertainties, stemming from unknown or incorrectly represented processes or input data. The former includes chemical reactions, transport and deposition processes, the latter includes emission data and meteorological fields. Nevertheless, the model is able to reproduce observed concentration levels and their spatiotemporal variation. The agreement between modelled and observed concentrations (see section 4.3) is in a range that is typical for regional CTMs (see e.g. Solazzo et al. (2012)). The deviations from the observed values can be interpreted as relative uncertainties in the modelled lockdown effects. During the lockdown between March and June, deviations between modelled and observed concentrations are often higher than the changes caused by the lockdown. Therefore, the results cannot be used to judge how accurate the estimated emission reductions are. It should be noted also that the simulations for 2016 and 2018 do not resemble the real situation during these years, because all emissions and chemical boundary conditions were for 2020.

### NO<sub>2</sub> concentrations

During the six weeks of the most stringent lockdown measures in Central Europe (16 March to 30 April), emission reductions caused NO<sub>2</sub> concentrations reductions between 15% and more than 50%. This is in good agreement with other studies (Velders et al., 2021; Menut et al., 2020; Gaubert et al., 2021) and also close to what was estimated from satellite observations. Bauwens et al. (2020) report columnar NO<sub>2</sub> reductions of approx. 20% around Hamburg, Frankfurt and Brussels, 28% for the area around Paris and 33 – 38% for Northern Italy. These reductions are almost independent of the meteorological situation, as can be seen in Fig 165 (top row). Differences in modelled NO<sub>2</sub> concentrations between 2020 and 2016 or 2018 show variations of more than 30%, but they are fluctuating in both directions on small spatial scales (see Fig. 154, top row). Larger areas with systematic differences are mainly found over sea and in areas with relatively low average concentrations, like in the western UK. It can be concluded that the NO<sub>2</sub> concentration reductions during the lockdown were dominated by the emission reductions and not very much by the meteorological situation. This is in agreement with the fact that NO<sub>2</sub> concentrations are spatially closely connected to the emission sources. NO<sub>2</sub> is quickly formed from NO after the latter was emitted into the atmosphere. It will then react further to form O<sub>3</sub> at daytime. Compared to O<sub>3</sub> and secondary PM, NO<sub>2</sub> is a rather short-lived gas with high spatial gradients and a clear annual cycle. However, as the situation in February 2020 shows, very unusual meteorological conditions can also cause large deviations from expected concentrations.

### O<sub>3</sub> concentrations

Ozone concentrations depend more strongly on weather conditions and on emissions of other precursors like VOCs. Therefore, meteorological variations from year to year might have a much stronger influence on average concentrations than the emission reductions during the lockdown. The six-weeks-average ozone concentrations vary by +/- 15% between 2020 and 2016 or 2018 (Fig 154, middle row) while the lockdown effects are mostly in the range of +/- 5% (Fig 165, middle row), except in densely populated areas. Weather conditions between 16

766 March and 30 April 2020 favoured relatively lower ozone concentrations in most parts of Central Europe when  
767 compared to 2016 and 2018. In the simulations, only areas in the western Alpine region show higher ozone in  
768 2020 (Fig 154, middle row). First of all, this is surprising because 2020 was comparably sunny and dry, which  
769 should favour ozone formation. The latter was also stated by Deroubaix et al. (2021) and Gaubert et al. (2021) in  
770 their studies about the COVID19-lockdown effects on air quality. However, advection of relatively clean air from  
771 Scandinavia into the North Eastern part of the model domain led to lower ozone concentrations particularly in the  
772 second half of April. A comparison of the meteorological effects on NO<sub>2</sub> and O<sub>3</sub> in Fig 154 also shows that NO<sub>2</sub>  
773 was relatively high and O<sub>3</sub> relatively low in 2020 in the English Channel, in south western UK and Belgium. The  
774 high pressure situation with relatively low wind speeds in 2020 resulted in efficient ozone destruction at night in  
775 areas with high NO emissions.

776 Lockdown effects on ozone might differ in sign under different meteorological conditions, as can be seen in Fig  
777 16. Lockdown-The emission reductions caused relative ozone increases in urban areas and throughout the northern  
778 part of the model domain, because these areas are VOC-limited regions. This was also reported by Menut et al.  
779 (2020) and Mertens et al. (2021). (Menut et al., 2020; Mertens et al., 2021) The effect is most pronounced in the  
780 second half of March and then decreases over time when VOC emissions, in particular from natural sources,  
781 increase (Fig. A7). In For northern Central Europe the small effects on ozone is is are connected with advection of  
782 clean air from north east. Lockdown effects on ozone might differ in sign under different meteorological  
783 conditions, as can be seen in Fig 15. For most parts of Central Europe, O<sub>3</sub> concentrations were decreased by  
784 lockdown measures. About 2-4% O<sub>3</sub> concentration reductions in most parts of Central Europe could have been  
785 expected with 2018 meteorological fields, when solar radiation was lower but more southerly winds prevailed in  
786 northern Central Europe. On the other hand, with 2016 meteorological conditions ozone changes would show  
787 similar patterns as 2020. Ozone chemistry depends on radiation, precipitation, atmospheric mixing and the  
788 availability of precursors in a complex way. The response of ozone concentrations to emission changes is therefore  
789 not straightforward to predict. Also long range transport, which was neglected here, may play role (see also  
790 Deroubaix et al. (2021) and Mertens et al. (2021)).

#### 791 **PM<sub>2.5</sub> concentrations**

792 PM<sub>2.5</sub> is another secondary pollutant that depends strongly on weather conditions, but emission reductions will  
793 primarily lead to concentration reductions (see Figures 132 and 143). However, the strength of this effect might  
794 also vary considerably with meteorological conditions. Fig 154 (bottom row) shows that the main lockdown period  
795 in 2020 was favourable for PM<sub>2.5</sub> formation in most parts of Central Europe, with often 20% to 50% higher PM<sub>2.5</sub>  
796 concentrations compared to other meteorological situations. An exception is the north eastern part of the model  
797 domain, where the meteorological situation in 2020 led to much lower PM<sub>2.5</sub> concentrations compared to 2018  
798 (more than 50% lower) and 2016 (20-40% lower). Similar to the situation for ozone, this is connected to the  
799 easterly and north easterly winds and the advection of clean air. Consequently, lockdown emission reductions had  
800 only very minor effects on PM<sub>2.5</sub> concentrations in 2020 in southern Sweden, Denmark, Poland and northern  
801 Germany.

802 Among the PM<sub>2.5</sub> components, particle bound nitrate is reduced strongest (Fig. A9-A11). Sulphate might even  
803 increase in some areas where ammonia becomes available when ammonium nitrate aerosol concentrations are  
804 reduced. Small amounts of additional ammonium sulphate can then be formed. Reduced VOC emissions are likely

805 ~~to cause also a decrease in secondary organic aerosol (SOA) formation, as proposed by Gaubert et al. (2021).~~  
806 ~~Given the uncertainties in SOA formation mechanisms in regional CTMs (Bessagnet et al., 2016), lockdown~~  
807 ~~effects on SOA were not investigated in this study.~~

808 Higher PM<sub>2.5</sub>- reductions would have been observed in most parts of Europe with 2016 and 2018 meteorological  
809 conditions. This can be interpreted in a way that the main lockdown period in 2020 was favourable for PM<sub>2.5</sub>  
810 formation in large parts of Europe leading to smaller relative PM<sub>2.5</sub> concentration reductions, given that the  
811 emission changes are the same.

812  
813 Summarized, it can be said that the effects of lockdown emission reductions depend strongly on the meteorological  
814 situation and that concentration changes because of weather conditions might be stronger than those of large  
815 emission changes during a six weeks period in spring. However, this mainly holds for the secondary pollutants O<sub>3</sub>  
816 and PM<sub>2.5</sub>, while the effects on NO<sub>2</sub> concentrations are less pronounced. Particularly changes in O<sub>3</sub> concentrations  
817 are difficult to predict because of the complex emission-chemistry-meteorology interactions.

## 818 7 Conclusions

819 ~~In this study, emission reductions during the first and most significant lockdown phase in Europe are estimated~~  
820 ~~from available mobility data, AIS ship position data and statistical data about industrial production and energy~~  
821 ~~use. They are applied to European emission data that is updated for 2020 following recent emission trends in~~  
822 ~~individual countries and sectors. Through meteorological and chemistry transport modelling with the COSMO-~~  
823 ~~CLM/CMAQ model system for Europe, and in higher spatial resolution for Central Europe, lockdown effects on~~  
824 ~~air pollutant concentrations are calculated. These are put into perspective with available observational data and~~  
825 ~~with modelled concentration changes from year to year that can be caused by varying meteorological conditions~~  
826 ~~for the same time of the year. The following conclusions can be drawn from this investigation.~~

827 Lockdown emission reductions in spring 2020 in Central Europe ~~were~~ significant, in particular those in traffic.  
828 Other sectors, like shipping, might be of regional importance, but emission changes for this sector are less certain.  
829 Aviation shows the largest relative reduction among the emission sectors considered, however the contribution to  
830 the total emissions reductions is small because of its low share in total NO<sub>x</sub> emissions. Consequently, strongest  
831 lockdown emissions reductions are seen for cities. The period with largely reduced emissions was limited to a few  
832 weeks and emissions increased again towards mid of 2020.

833 In absolute numbers, concentration reductions ~~were~~ strongest for NO<sub>2</sub> in cities and for larger areas in the Po  
834 valley with more than 6 µg/m<sup>3</sup> for a two weeks average in the second half of March. Northern Italy also show~~ed~~  
835 the strongest relative decline with more than 50%. Rural areas in Germany, Poland and the Czech Republic  
836 show~~ed~~ the lowest reductions between 10% and 20%.

837 Ozone concentrations were often reduced, but not in cities and not in northern Europe between mid of March and  
838 beginning of April. This can be explained by reduced titration in cities (NO - O<sub>3</sub> reactions that destroy ozone)  
839 during the first phase of the lockdown, when NO emissions were lowest. ~~However, when VOC emissions increase~~  
840 ~~in spring, most regions turn into NO<sub>x</sub>-limited areas, which means that ozone concentrations also decrease when~~  
841 ~~NO<sub>x</sub> emissions decrease.~~ The O<sub>3</sub> concentration changes ~~were~~ around +/- 5% which is much less than the NO<sub>2</sub>  
842 changes. The impacts of meteorological conditions can be much larger and the temporary O<sub>3</sub> increase in north

Formatiert: Tiefgestellt

Formatiert: Tiefgestellt

Formatiert: Tiefgestellt

843 eastern Europe in March would not have taken place under meteorological conditions as they were present in the  
844 years 2016 and 2018.

845 PM<sub>2.5</sub> concentrations ~~were~~ also decreased because of the lockdown emissions reductions, but the magnitude ~~was~~  
846 much smaller than for NO<sub>2</sub>, only between 2% and 10%. ~~Particle bound nitrate contributes most to this effect.~~  
847 Again, concentration changes can be much larger due to meteorological conditions. The reductions in 2020 were  
848 relatively lower compared to the effects with 2016 and 2018 meteorological conditions.

849 Because the meteorological effects on concentrations of O<sub>3</sub> and PM<sub>2.5</sub> are larger than the lockdown emission  
850 reduction effects, it is difficult to judge or even quantify emission reduction effects by observations and  
851 comparison with previous years, only. For NO<sub>2</sub>, this is different, but in exceptional situations, like in February  
852 2020, NO<sub>2</sub> can also be strongly influenced by meteorological conditions and lead to lower concentrations than in  
853 March during lockdown conditions.

854 Meteorological and chemistry transport models need to be applied to investigate the effects of emission reductions  
855 and separate them from meteorological effects. Although these models have deficiencies and systematic errors,  
856 e.g. underestimation of NO<sub>2</sub> and PM<sub>2.5</sub> concentrations, the impacts of emission changes caused by the lockdown  
857 can be quantified. ~~The effects in absolute numbers might be lower by the same magnitude as the model~~  
858 ~~underestimates NO<sub>2</sub> and PM<sub>2.5</sub>.~~ The model accuracy is not sufficient to judge the correctness of the emission  
859 reduction estimates, however, the calculated NO<sub>2</sub> reductions agree well with estimations from ground based and  
860 satellite observations for Central Europe.

861 The emission reductions for several weeks during the first COVID-19 lockdown in Europe were the largest since  
862 decades. They can be seen as a huge test for emission reductions that could be achieved with significantly reduced  
863 car traffic and air traffic. The reductions resulted in much lower NO<sub>2</sub> concentrations, particularly in cities, but the  
864 effects on secondary pollutants like ozone and PM<sub>2.5</sub> were limited and are hard to predict. The latter holds  
865 particularly for ozone that might even increase in some areas when traffic emissions are decreased. ~~Year-to-year~~  
866 ~~variability caused by meteorological conditions has larger impacts on O<sub>3</sub> and PM<sub>2.5</sub> than the lockdown emission~~  
867 ~~changes. This implies that~~ systematic changes in prevailing weather situations that might appear due to climate  
868 change could mask effects of emission reductions on secondary pollutants. The relatively short duration of strong  
869 lockdown measures also results in limited effects on annual average NO<sub>2</sub> concentrations. Depending on location,  
870 only between 3% and 15% lower values could be reached.

## 871 Acknowledgements

872 The Community Air Quality Modeling System (CMAQ) is developed and maintained by the US EPA. Its use is  
873 gratefully acknowledged. ~~J. Kuenen from TNO, Department of Climate, Air and Sustainability, is acknowledged~~  
874 ~~for the provision of NMVOC splits for use with the CAMS-REG-AP emission inventory.~~

875 We thank to the weather mast group of the Meteorological Institute at the University of Hamburg, who delivered  
876 data from tower site Wettermast Hamburg.

877 We also thank the German Maritime and Hydrographic Agency for supporting us with AIS data taken in  
878 Bremerhaven, Hamburg and Kiel.

Formatiert: Schriftart: (Standard) Times New Roman, 10 Pt.

879 **Author contribution**

880 VM developed the idea, designed and supervised the study, evaluated part of the model results, prepared the  
881 manuscript and wrote most of the text. MQ co-designed the study, wrote most of the text about the meteorological  
882 situation and provided interpretations of the meteorology-chemistry interactions. JAA helped in designing the  
883 study, performed CMAQ model runs and provided code for the emission data preparation. RB developed the  
884 Lockdown Adjustment Factors, extrapolated emission data, and wrote the section about the emission data. LF  
885 performed CMAQ model runs, evaluated CMAQ model results and observation data and provided most of the  
886 plots. RP performed COSMO model runs, provided information for the meteorological data interpretation, wrote  
887 the text about the COSMO setup and part of the text about the meteorological situation, and analysed COSMO  
888 model results. JF developed emission extrapolation factors, and provided interpretation of the observational data.  
889 DS analysed AIS data and calculated ship emission LAFs. EML collected and analysed observational data and  
890 provided data interpretation. MR helped in designing the study, analysed and interpreted observational data for  
891 suburban stations. RW collected data on aviation emissions, provided LAFs for aviation and contributed to the  
892 discussion of the results

893 **Code and data availability**

894 The CMAQ model code is available through the CMAS Center <https://www.cmascenter.org/cmaq/>. The COSMO-  
895 CLM model is documented and available for members of the COSMO-CLM community at  
896 <https://wiki.coast.hereon.de/clmcom> . Lockdown adjustment factors (LAF) and projection factors (PF) as well as  
897 CMAQ model results are available upon request.

898 **Competing interests**

899 The authors declare no conflict of interest.  
900

901 **Appendix A**

902 **A1 Emission data**

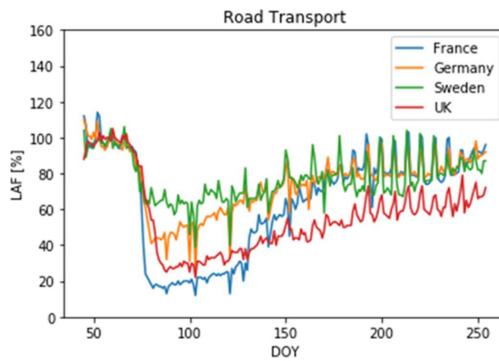
903 **Table A1: Overview on available emission reduction information for countries in the investigated domain during the**  
904 **lockdown applied in this study**

Country or Ocean Area	A_PublicPower	B_Industry	F_RoadTransport	G_Shipping	G_Shipping_Inland	H_Aviation
Albania					x	x
Austria	x	x	x		x	x
Baltic Sea				x		
Belarus			x		x	x
Belgium	x	x	x		x	x

Bosnia and Herzegovina	x		x		x	x
Bulgaria	x	x	x		x	x
Croatia	x	x	x		x	x
Cyprus	x				x	x
Czech Republic	x	x	x		x	x
Denmark	x	x	x		x	x
Estonia	x		x		x	x
Finland	x	x	x		x	x
France	x	x	x		x	x
Germany	x	x	x		x	x
Greece	x		x		x	x
Hungary	x	x	x		x	x
Iceland					x	x
Ireland	x		x		x	x
Italy	x	x	x		x	x
Latvia	x		x		x	x
Liechtenstein			x		x	
Lithuania	x		x		x	x
Luxembourg	x	x	x		x	x
Malta	x		x		x	x
Moldova			x		x	x
Montenegro	x				x	x
Netherlands	x	x	x		x	x
North Macedonia	x		x		x	x
North Sea				x		
Norway	x		x		x	x
Poland	x	x	x		x	x
Portugal	x	x	x		x	x
Romania	x	x	x		x	x
Russia			x		x	x
Serbia	x		x		x	x
Slovakia	x	x	x		x	x
Slovenia	x	x	x		x	x
Spain	x	x	x		x	x
Sweden	x		x		x	x
Switzerland	x		x		x	x

Turkey	x		x		x	x
United Kingdom	x	x	x		x	x
Ukraine			x		x	x

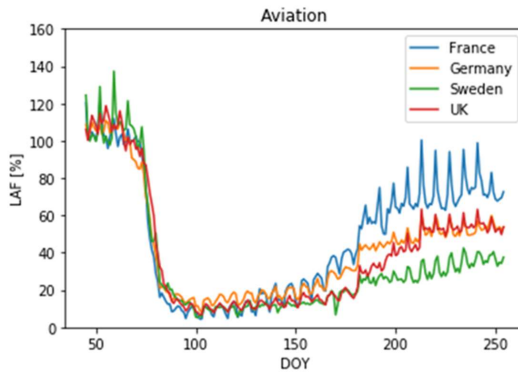
905



906

907 **Figure A1: Daily values for Lockdown Adjustment Factors (in %) for the sector F\_RoadTransport based on transit**  
 908 **data from the Google Mobility Reports.**

909



910

911 **Figure A2: Daily values for Lockdown Adjustment Factors (in %) for the sector H\_Aviation based on Eurocontrol**  
 912 **data.**

913 **A2 Meteorological situation**

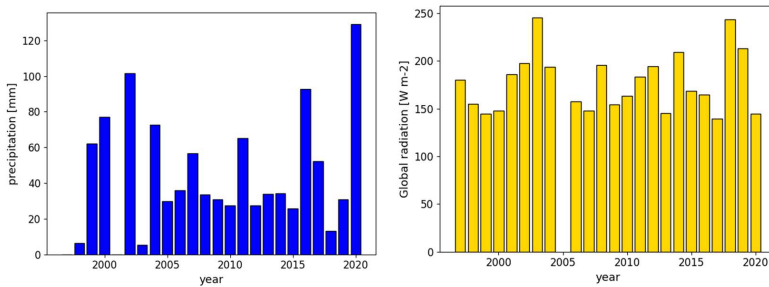
914 **Table A2: GWL classification for the period 1 February 2020 – 31 May 2020**

Date range	GWL
01.02. - 02.02.	Cyclonic Westerly
03.02. - 05.02.	Cyclonic North-Westerly



06.02. - 08.02.	High over Central Europe
09.02. - 12.02.	Cyclonic Westerly
13.02. - 16.02.	Anticyclonic South-Westerly
17.02. - 25.02.	Cyclonic Westerly
26.02. - 28.02.	Cyclonic North-Westerly
29.02. - 03.03.	Trough over Western Europe
04.03. - 06.03.	South-Shifted Westerly
07.03. - 09.03.	Maritime Westerly (Block E. Europe)
10.03. - 12.03.	Cyclonic Westerly
13.03. - 16.03.	Zonal Ridge across Central Europe
17.03. - 20.03.	Anticyclonic Westerly
21.03. - 26.03.	Scandinavian High Ridge C. Europe
27.03. - 29.03.	Anticyclonic North-Easterly
30.03. - 01.04.	Anticyclonic Northerly
02.04. - 04.04.	Anticyclonic North-Westerly
05.04. - 08.04.	Anticyclonic Southerly
09.04. - 11.04.	High over Central Europe
12.04.	undefined
13.04. - 15.04.	High over the British Isles
16.04. - 18.04.	Icelandic High Ridge C. Europe
19.04. - 23.04.	High Scandinavia-Iceland Ridge C. Europe
24.04. - 26.04.	Anticyclonic North-Westerly
27.04. - 29.04.	South-Shifted Westerly
30.04. - 02.05.	Cyclonic Westerly
03.05. - 05.05.	Anticyclonic Northerly
06.05. - 08.05.	High over Central Europe
09.05. - 12.05.	Icelandic High Trough C. Europe
13.05. - 15.05.	Anticyclonic North-Westerly
16.05. - 18.05.	Zonal Ridge across Central Europe
19.05. - 23.05.	High over Central Europe
24.05. - 27.05.	Anticyclonic Northerly
28.05. - 30.05.	Anticyclonic North-Easterly
31.05. - 02.06.	High Scandinavia-Iceland Ridge C. Europe

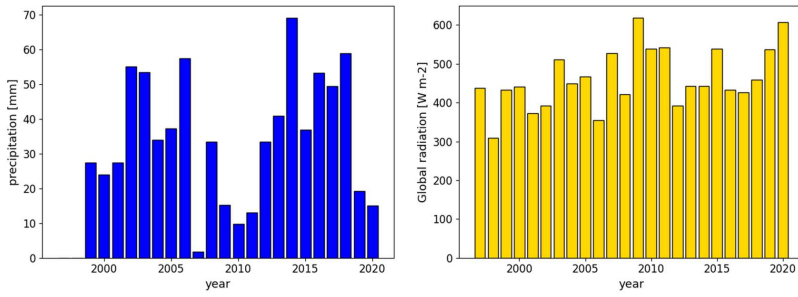
915



916

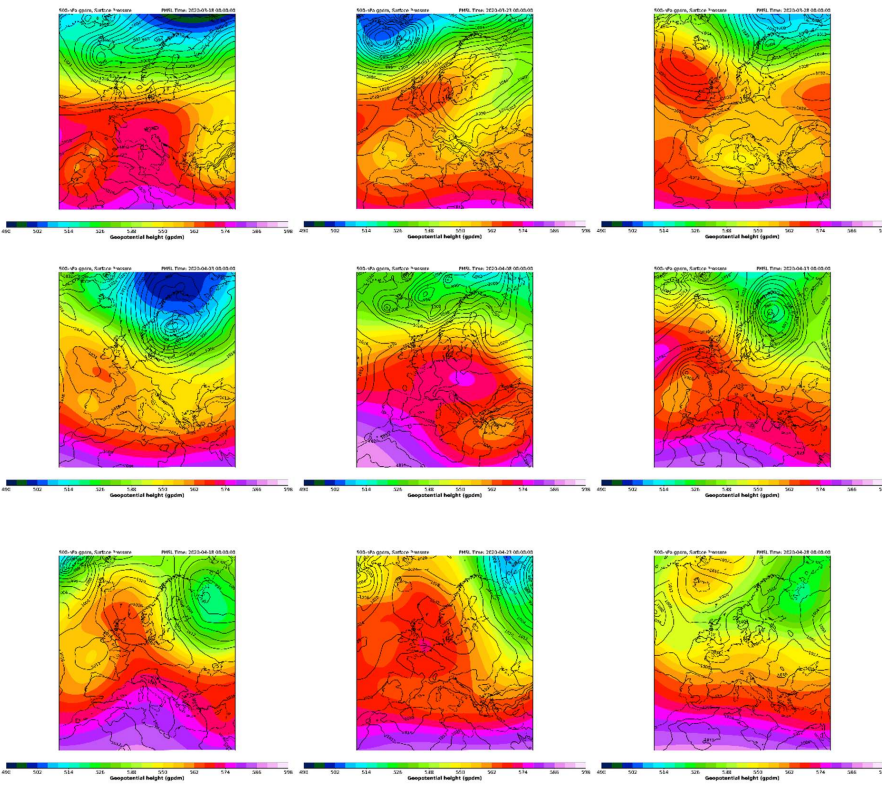
917 **Figure A3: Time series of the monthly accumulated precipitation and mean solar irradiance between 10 and 14 UTC**  
918 **at the Wettermast Hamburg for February from 1997-2020.**

919



920 **Figure A4: Time series of the monthly accumulated precipitation and mean solar irradiance between 10 and 14 UTC**  
921 **at the Wettermast Hamburg for April from 1997-2020.**  
922  
923

924



925

926

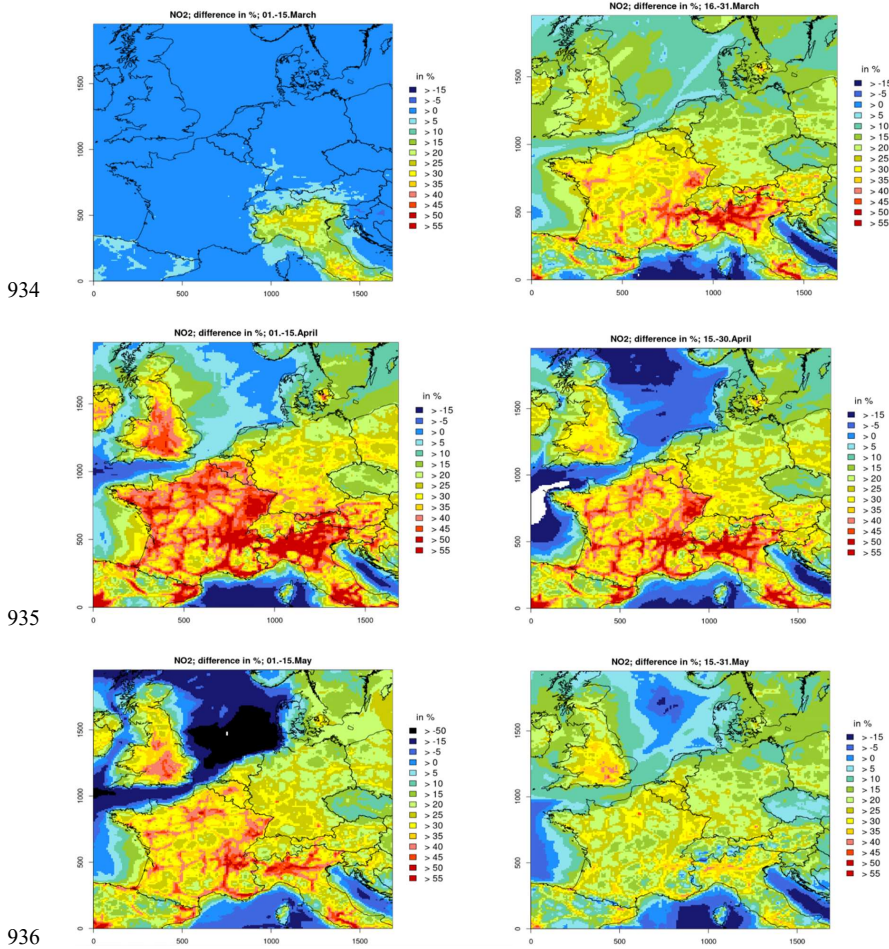
927

928 Figure A5: 500 hPa geopotential heights (in gpm) and surface pressure (in hPa) for 4-days time segments in March  
 929 and April 2020 according to the COSMO simulations. The geopotential heights are averaged over 4 days, displayed  
 930 surface pressure distributions are representative snap shots within those time segments.

931

932 A3 COVID-19 lockdown effects

933



934

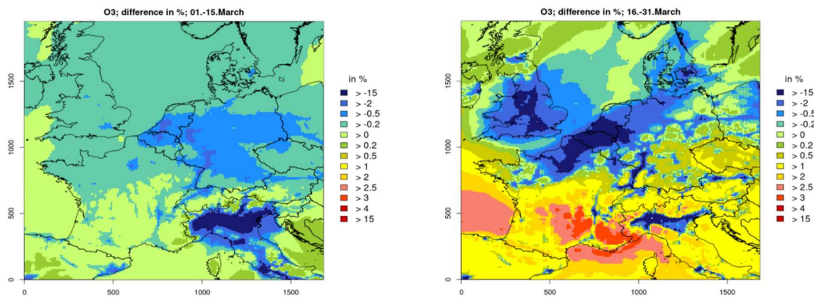
935

936

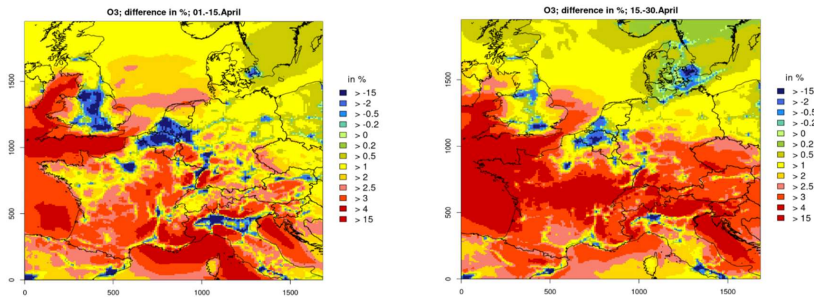
937 Figure A6: CMAQ results for relative NO2 concentrations reductions due to lockdown measures (noCOV – COV run)  
 938 in Central Europe between 1 March and 31 May 2020 in half-monthly intervals; positive values denote reductions.

939

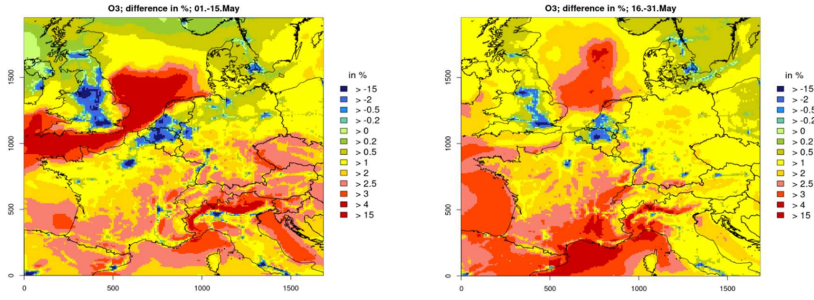
940



941



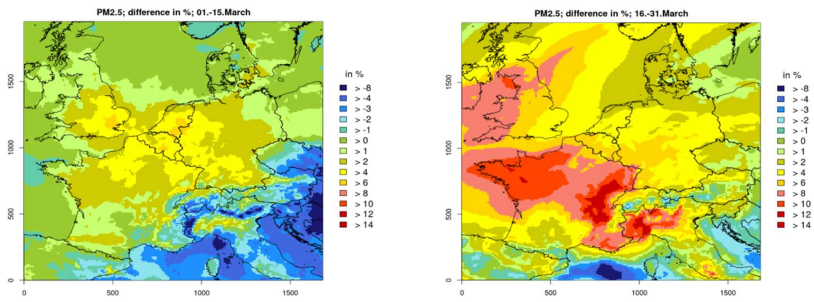
942



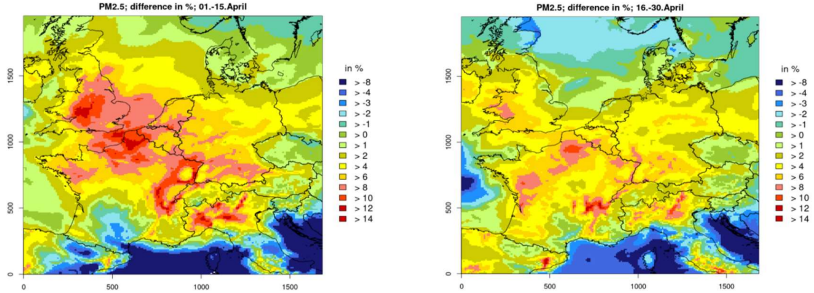
943 **Figure A7: CMAQ results for relative O<sub>3</sub> concentrations reductions due to lockdown measures (noCOV – COV run)**  
944 **in Central Europe between 1 March and 31 May 2020 in half-monthly intervals; positive values denote reductions.**

945

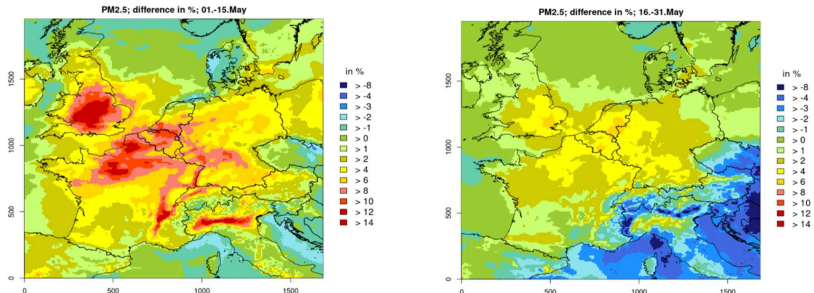
946



947

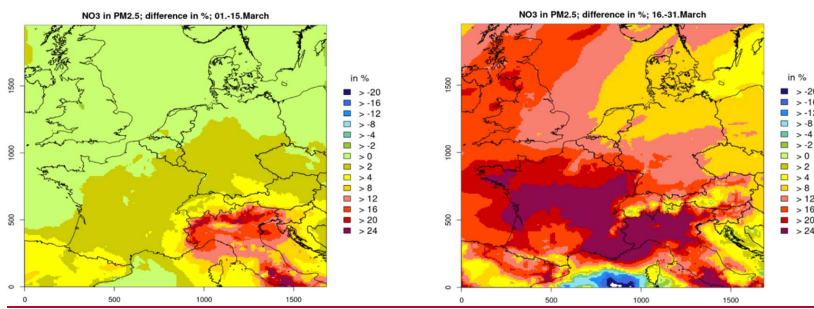


948



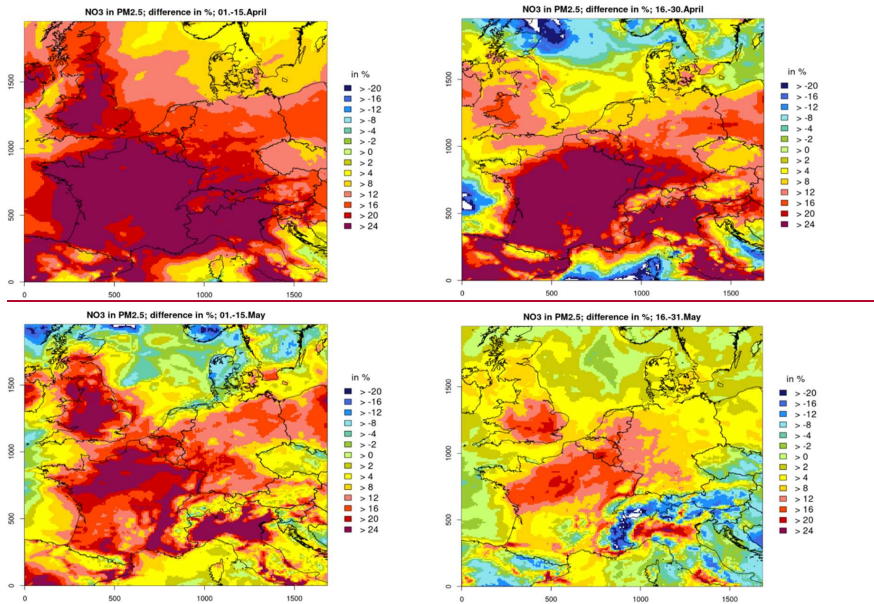
949 Figure A8: CMAQ results for relative PM2.5 concentrations reductions due to lockdown measures (noCOV – COV  
950 run) in Central Europe between 1 March and 31 May 2020 in half-monthly intervals; positive values denote reductions.

951



952

953

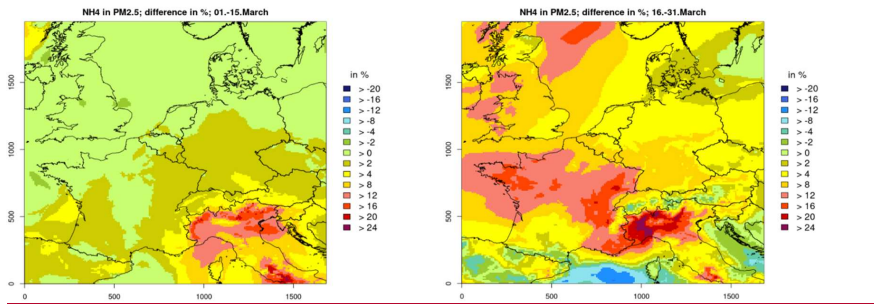


954

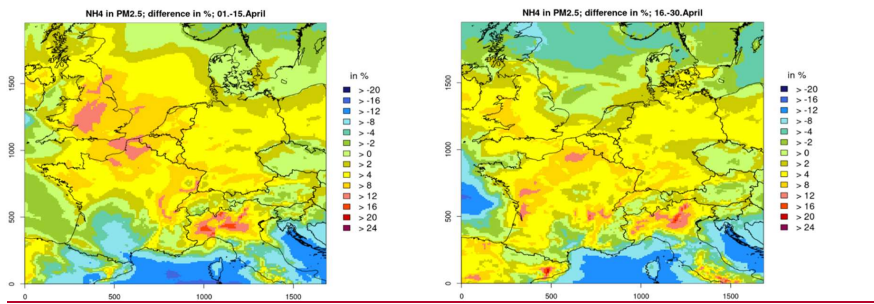
955 Figure A9: CMAQ results for relative particulate nitrate (NO<sub>3</sub>) concentrations reductions due to lockdown measures  
956 (noCOV – COV run) in Central Europe between 1 March and 31 May 2020 in half-monthly intervals; positive values  
957 denote reductions.

958

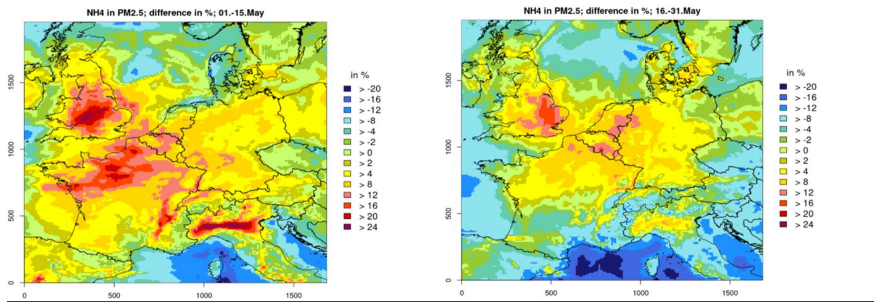
959



960



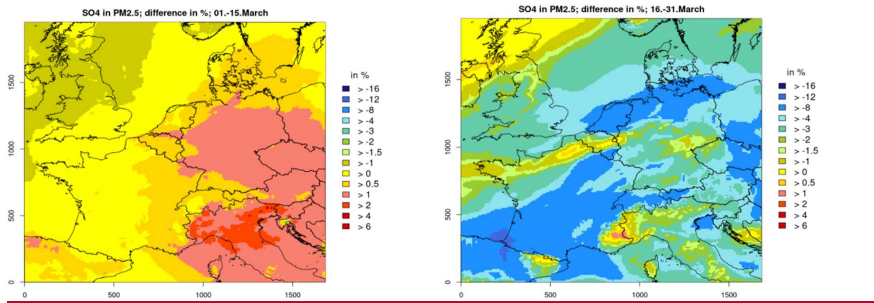
961



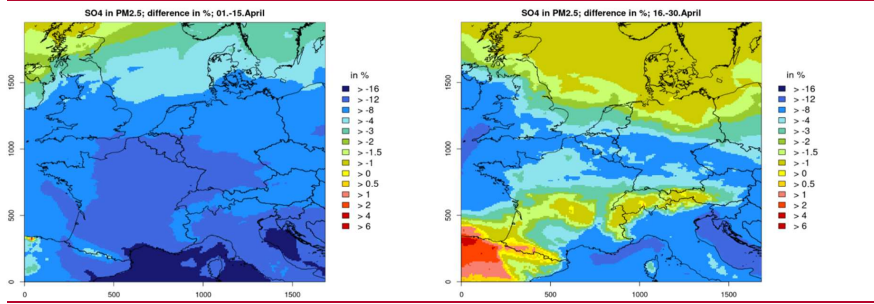
962 **Figure A10: CMAQ results for relative particulate ammonium (NH<sub>4</sub><sup>+</sup>) concentrations reductions due to lockdown**  
963 **measures (noCOV – COV run) in Central Europe between 1 March and 31 May 2020 in half-monthly intervals; positive**  
964 **values denote reductions.**

965

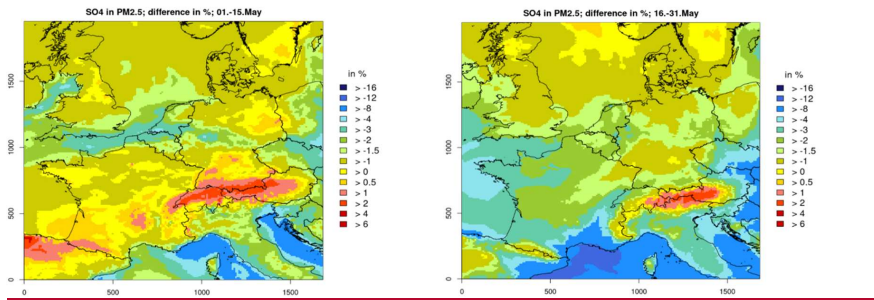
966



967



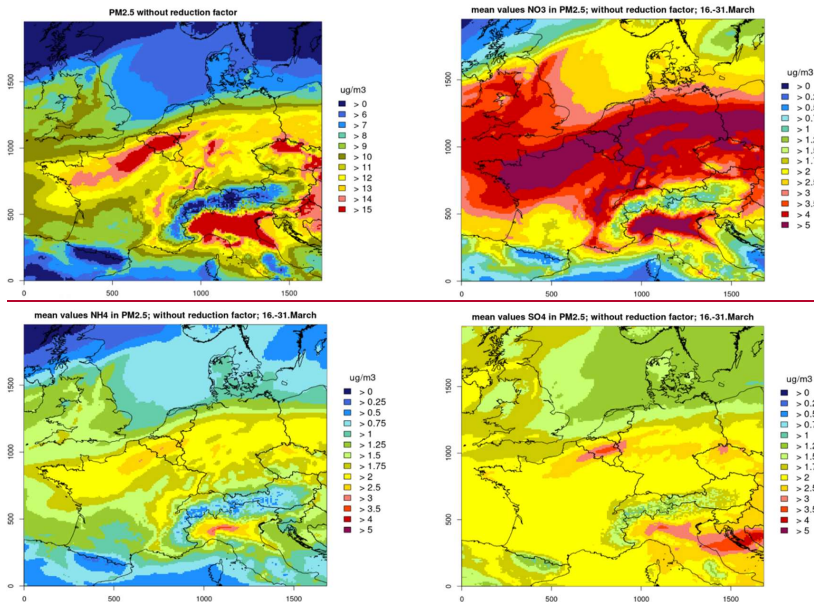
968



969 **Figure A11: CMAQ results for relative particulate sulfate ( $\text{SO}_4^{2-}$ ) concentrations reductions due to lockdown measures**  
970 **(noCOV – COV run) in Central Europe between 1 March and 31 May 2020 in half-monthly intervals; positive values**  
971 **denote reductions.**

972





973

974

975

976

**Figure A12: CMAQ results for concentrations of PM2.5 and its components nitrate, ammonium and sulphate in Central Europe between 16 March and 31 March 2020.**

977

978

**A4 Meteorological differences 2020 versus 2016 and 2018**

979

**Discussion**

980

In 2020 the geopotential height at 500 hPa over the British Isles and the North Sea was significantly higher compared to that in 2016, especially from 1 April onward. This resulted in a constellation which favours blocking in 2020. Near surface high pressure systems were amplified and more persistent and weak wind conditions and a more continental flow dominate. In 2016 stronger winds of Atlantic origin occasionally were observed. In 2020 precipitation was considerably lower compared to 2016. In most parts of the study region solar radiation was clearly higher in 2020, especially over Central Europe up to the British Isles.

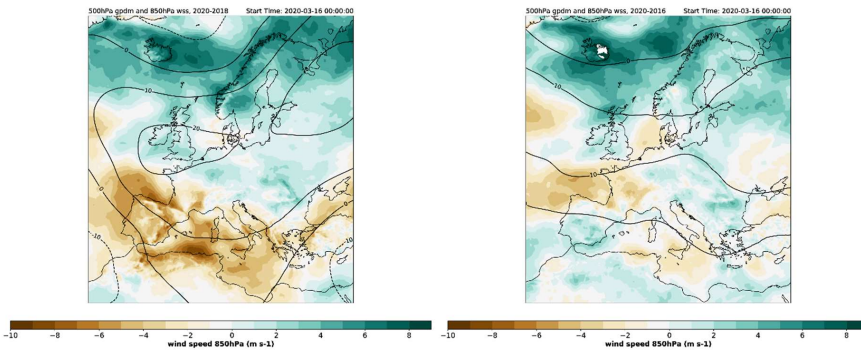
986

Much of what has been said concerning the blocking condition in 2020 holds as well when compared to 2018.

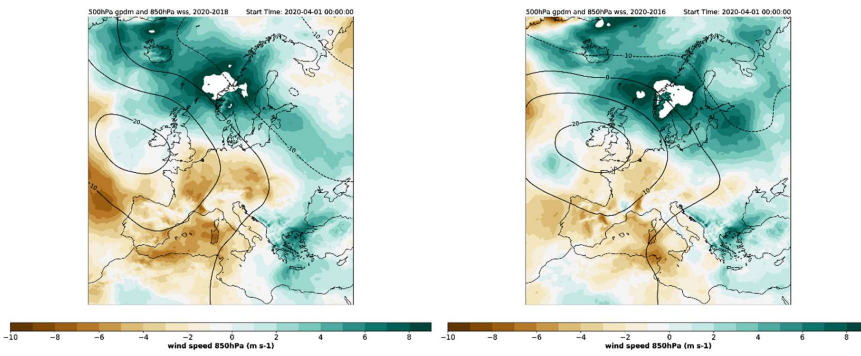
987

The year 2020 also was much drier and incoming solar radiation was more intense. In 2018 winds had a more easterly to south-easterly component. The spatial and temporal distribution and the absolute values of the meteorological parameters were slightly different in 2018 compared to 2016 (see Fig. A13- A15), so this year became an additional choice for the evaluation of meteorological influences.

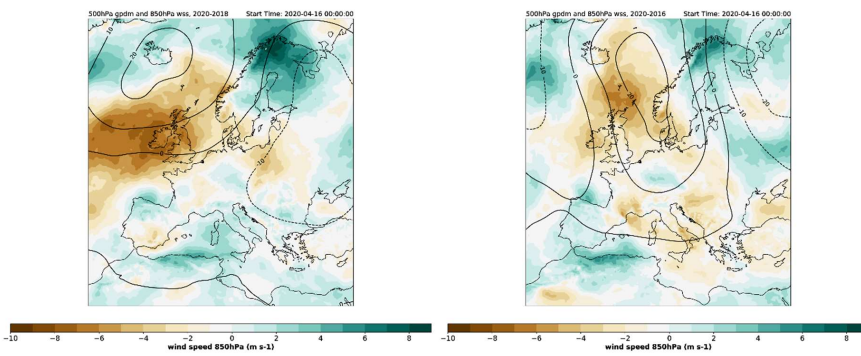
991



992



993

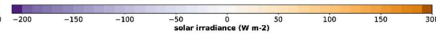
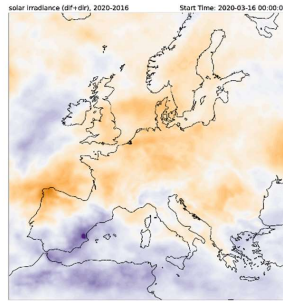
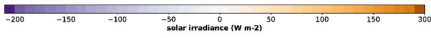
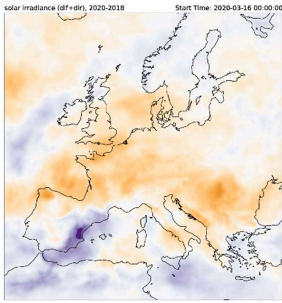


994

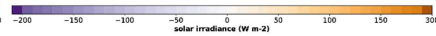
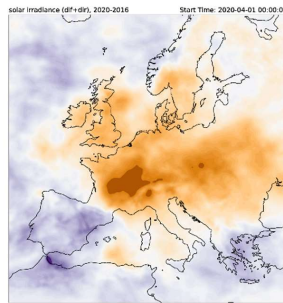
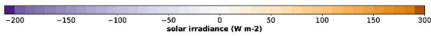
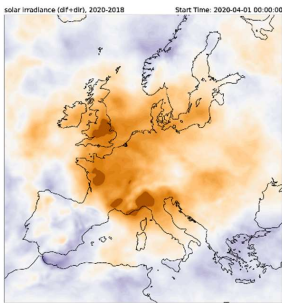
995 **Figure A139:** Geopotential height at 500 hPa (in gpdm, isolines) and windspeed at 850 hPa (in m/s, color code):  
 996 Differences between 2020 and 2018 (left column) and 2020 and 2016 (right column) for the half month-periods 16 march  
 997 – 31 March (top), 1 April – 15 April (middle) and 16 April – 30 April (bottom).

998

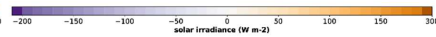
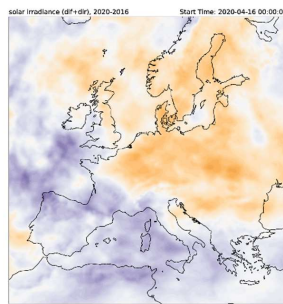
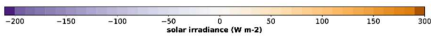
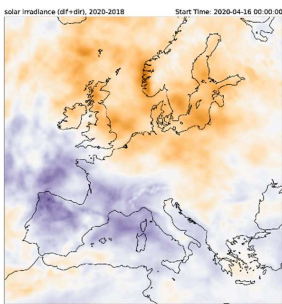
999



1000



1001

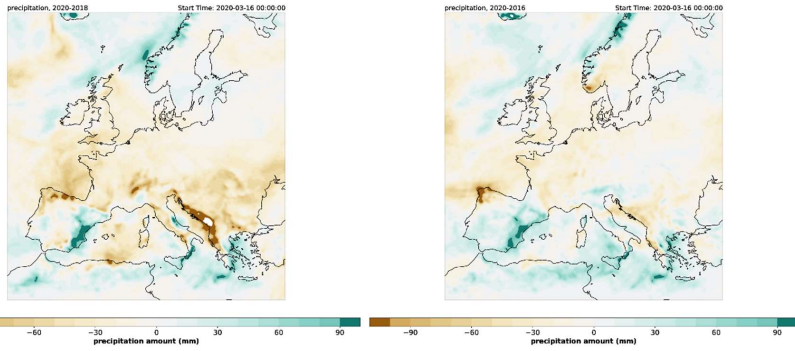


1002

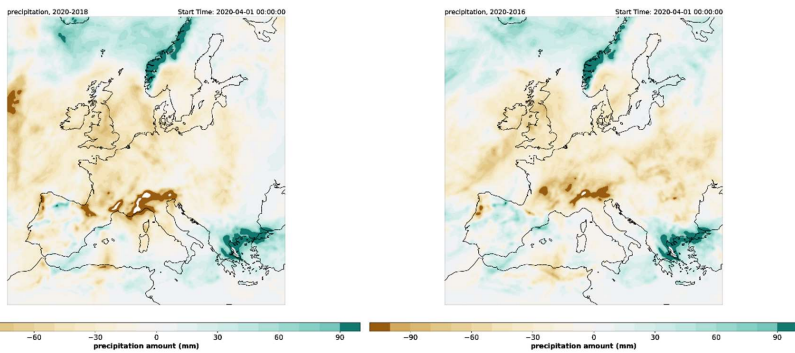
1003 **Figure A140:** Solar irradiance (in  $W/m^2$ , color code): Differences between 2020 and 2018 (left column) and 2020 and  
 1004 2016 (right column) for the half month-periods 16 March – 31 March (top), 1 April – 15 April (middle) and 16 April –  
 1005 30 April (bottom).

1006

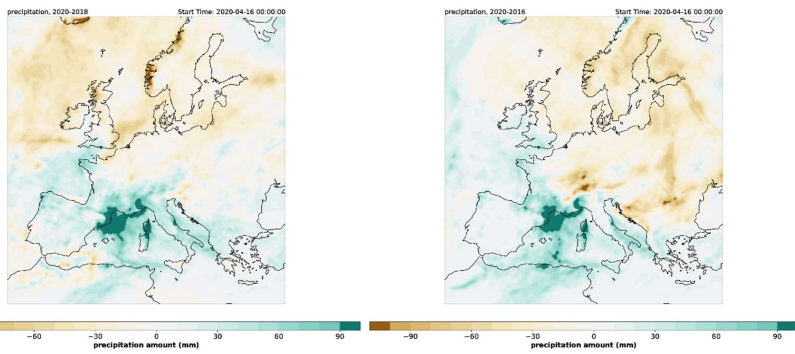
1007



1008



1009



1010

1011 **Figure A151:** Accumulated precipitation (in mm, color code): Differences between 2020 and 2018 (left column) and  
 1012 2020 and 2016 (right column) for the half month-periods 16 March – 31 March (top), 1 April – 15 April (middle) and  
 1013 16 April – 30 April (bottom).

1014

1015 **References**

1016

1017 [Amouei Torkmahalleh, M., Akhmetvaliyeva, Z., Omran, A. D., Faezeh Darvish Omran, F., Kazemitabar, M.,](#)  
1018 [Naseri, M., Naseri, M., Sharifi, H., Malekipirbazari, M., Kwasi Adotey, E., Gorjinezhad, S., Eghtesadi, N.,](#)  
1019 [Sabanov, S., Alastuey, A., de Fátima Andrade, M., Buonanno, G., Carbone, S., Cárdenas-Fuentes, D. E., Cassee,](#)  
1020 [F. R., Dai, Q., Henríquez, A., Hopke, P. K., Keronen, P., Khwaja, H. A., Kim, J., Kulmala, M., Kumar, P., Kushta,](#)  
1021 [J., Kuula, J., Massagué, J., Mitchell, T., Mooibroek, D., Morawska, L., Niemi, J. V., Ngagine, S. H., Norman, M.,](#)  
1022 [Oyama, B., Oyola, P., Öztürk, F., Petäjä, T., Querol, X., Rashidi, Y., Reyes, F., Ross-Jones, M., Salthammer, T.,](#)  
1023 [Savvides, C., Stabile, L., Sjöberg, K., Söderlund, K., Sunder Raman, R., Timonen, H., Umezawa, M., Viana, M.,](#)  
1024 [and Xie, S.: Global Air Quality and COVID-19 Pandemic: Do We Breathe Cleaner Air?, Aerosol and Air Quality](#)  
1025 [Research, 21, 200567, 10.4209/aaqr.200567, 2021.](#)  
1026 [Baldauf, M., Seifert, A., Forstner, J., Majewski, D., Raschendorfer, M., and Reinhardt, T.: Operational](#)  
1027 [Convective-Scale Numerical Weather Prediction with the COSMO Model: Description and Sensitivities, Monthly](#)  
1028 [Weather Review, 139, 3887-3905, 10.1175/mwr-d-10-05013.1, 2011.](#)  
1029 [Baret, F., Weiss, M., Lacaze, R., Camacho, F., Makhmara, H., Pacholczyk, P., and Smets, B.: GEOV1: LAI and](#)  
1030 [FAPAR essential climate variables and FCOVER global time series capitalizing over existing products. Part1:](#)  
1031 [Principles of development and production, Remote Sensing of Environment, 137, 299-309,](#)  
1032 [10.1016/j.rse.2012.12.027, 2013.](#)  
1033 [Bauwens, M., Compernelle, S., Stavrakou, T., Muller, J. F., van Gent, J., Eskes, H., Levelt, P. F., van der, A. R.,](#)  
1034 [Veeffkind, J. P., Vlietinck, J., Yu, H., and Zehner, C.: Impact of coronavirus outbreak on NO2 pollution assessed](#)  
1035 [using TROPOMI and OMI observations, Geophys Res Lett, e2020GL087978, 10.1029/2020GL087978, 2020.](#)  
1036 [Bessagnet, B., Pirovano, G., Mircea, M., Cuvelier, C., Aulinger, A., Calori, G., Ciarelli, G., Manders, A., Stern,](#)  
1037 [R., Tsyro, S., Vivanco, M. G., Thunis, P., Pay, M. T., Colette, A., Couvidat, F., Meleux, F., Rouil, L., Ung, A.,](#)  
1038 [Aksoyoglu, S., Baldasano, J. M., Bieser, J., Briganti, G., Cappelletti, A., D'Isidoro, M., Finardi, S., Kranenburg,](#)  
1039 [R., Silibello, C., Carnevale, C., Aas, W., Dupont, J. C., Fagerli, H., Gonzalez, L., Menut, L., Prevot, A. S. H.,](#)  
1040 [Roberts, P., and White, L.: Presentation of the EURODELTA III intercomparison exercise - evaluation of the](#)  
1041 [chemistry transport models' performance on criteria pollutants and joint analysis with meteorology, Atmospheric](#)  
1042 [Chemistry and Physics, 16, 12667-12701, 10.5194/acp-16-12667-2016, 2016.](#)  
1043 [Bieser, J., Aulinger, A., Matthias, V., Quante, M., and Builtjes, P.: SMOKE for Europe - adaptation, modification](#)  
1044 [and evaluation of a comprehensive emission model for Europe, Geoscientific Model Development, 3, 949-1007,](#)  
1045 [2010.](#)  
1046 [Bieser, J., Aulinger, A., Matthias, V., Quante, M., and Denier van der Gon, H. A. C.: Vertical emission profiles](#)  
1047 [for Europe based on plume rise calculations, Environmental Pollution, 159, 2935-2946, 2011.](#)  
1048 [Bissolli, P., and Dittmann, E.: The objective weather type classification of the German Weather Service and its](#)  
1049 [possibilities of application to environmental and meteorological investigations, Meteorologische Zeitschrift, 10,](#)  
1050 [253-260, 10.1127/0941-2948/2001/0010-0253, 2001.](#)  
1051 [Brümmer, B., and Schultze, M.: Analysis of a 7-year low-level temperature inversion data set measured at the 280](#)  
1052 [m high Hamburg weather mast, Meteorologische Zeitschrift, 24, 481-494, 10.1127/metz/2015/0669, 2015.](#)

**Formatiert:** Standard, Block, Zeilenabstand: 1,5 Zeilen

**Feldfunktion geändert**

**Formatiert:** Schriftart: (Standard) Times New Roman, 10 Pt.

1053 Byun, D., and Schere, K. L.: Review of the Governing Equations, Computational Algorithms, and Other  
1054 Components of the Models-3 Community Multiscale Air Quality (CMAQ) Modeling System, *Applied Mechanics*  
1055 *Reviews*, 59, 51-77, 2006.

1056 Byun, D. W., and Ching, J. K. S.: Science Algorithms of the EPA Models-3 Community Multiscale Air Quality  
1057 Modeling System, 1999.

1058 Collivignarelli, M. C., Abba, A., Caccamo, F. M., Bertanza, G., Pedrazzani, R., Baldi, M., Ricciardi, P., and  
1059 Miino, M. C.: Can particulate matter be identified as the primary cause of the rapid spread of CoViD-19 in some  
1060 areas of Northern Italy?, *Environmental Science and Pollution Research*, 10.1007/s11356-021-12735-x, 2020.

1061 Denier van der Gon, H. A. C., Hendriks, C., Kuenen, J., Segers, A., and Visschedijk, A.: Description of current  
1062 temporal emission patterns and sensitivity of predicted AQ for temporal emission patterns EU FP7 MACC  
1063 deliverable report D\_D-EMIS\_1.3, 2011.

1064 Deroubaix, A., Brasseur, G., Gaubert, B., Labuhn, I., Menut, L., Siour, G., and Tuccella, P.: Response of surface  
1065 ozone concentration to emission reduction and meteorology during the COVID-19 lockdown in Europe,  
1066 *Meteorological Applications*, 28, e1990, <https://doi.org/10.1002/met.1990>, 2021.

1067 Doms, G., and Schättler, U.: A Description of the Nonhydrostatic Regional Model LM. Part I: Dynamics and  
1068 Numerics, 2002.

1069 Doms, G., Foerstner, J., Heise, E., Herzog, H. J., Mrionow, D., Raschendorfer, M., Reinhart, T., Ritter, B.,  
1070 Schrodin, R., Schulz, J. P., and Vogel, G.: A Description of the Nonhydrostatic Regional COSMO Model. Part II:  
1071 Physical Parameterization, 2011.

1072 Doumbia, T., Granier, C., Elguindi, N., Bouarar, I., Darras, S., Brasseur, G., Gaubert, B., Liu, Y., Shi, X.,  
1073 Stavrakou, T., Tilmes, S., Lacey, F., Deroubaix, A., and Wang, T.: Changes in global air pollutant emissions  
1074 during the COVID-19 pandemic: a dataset for atmospheric chemistry modeling, *Earth Syst. Sci. Data Discuss.*,  
1075 2021, 1-26, 10.5194/essd-2020-348, 2021.

1076 Forster, P. M., Forster, H. I., Evans, M. J., Gidden, M. J., Jones, C. D., Keller, C. A., Lamboll, R. D., Quéré, C.  
1077 L., Rogelj, J., Rosen, D., Schleussner, C.-F., Richardson, T. B., Smith, C. J., and Turnock, S. T.: Current and  
1078 future global climate impacts resulting from COVID-19, *Nature Climate Change*, 10, 913-919, 10.1038/s41558-  
1079 020-0883-0, 2020.

1080 Gaubert, B., Bouarar, I., Doumbia, T., Liu, Y., Stavrakou, T., Deroubaix, A., Darras, S., Elguindi, N., Granier, C.,  
1081 Lacey, F., Müller, J.-F., Shi, X., Tilmes, S., Wang, T., and Brasseur, G. P.: Global Changes in Secondary  
1082 Atmospheric Pollutants During the 2020 COVID-19 Pandemic, *Journal of Geophysical Research: Atmospheres*,  
1083 126, e2020JD034213, <https://doi.org/10.1029/2020JD034213>, 2021.

1084 Gelaro, R., McCarty, W., Suarez, M. J., Todling, R., Molod, A., Takacs, L., Randles, C. A., Darmenov, A.,  
1085 Bosilovich, M. G., Reichle, R., Wargan, K., Coy, L., Cullather, R., Draper, C., Akella, S., Buchard, V., Conaty,  
1086 A., da Silva, A. M., Gu, W., Kim, G. K., Koster, R., Lucchesi, R., Merkova, D., Nielsen, J. E., Partyka, G., Pawson,  
1087 S., Putman, W., Rienecker, M., Schubert, S. D., Sienkiewicz, M., and Zhao, B.: The Modern-Era Retrospective  
1088 Analysis for Research and Applications, Version 2 (MERRA-2), *Journal of Climate*, 30, 5419-5454, 10.1175/jcli-  
1089 d-16-0758.1, 2017.

1090 Gkatzelis, G. I., Gilman, J. B., Brown, S. S., Eskes, H., Gomes, A. R., Lange, A. C., McDonald, B. C., Peischl, J.,  
1091 Petzold, A., Thompson, C. R., and Kiendler-Scharr, A.: The global impacts of COVID-19 lockdowns on urban

**Formatiert:** Schriftart: (Standard) Times New Roman, 10 Pt.

**Formatiert:** Schriftart: (Standard) Times New Roman, 10 Pt.

1092 air pollution: A critical review and recommendations, *Elementa: Science of the Anthropocene*, 9,  
1093 10.1525/elementa.2021.00176, 2021.

1094 Goldberg, D. L., Anenberg, S. C., Griffin, D., McLinden, C. A., Lu, Z., and Streets, D. G.: Disentangling the  
1095 Impact of the COVID-19 Lockdowns on Urban NO<sub>2</sub> From Natural Variability, *Geophysical Research Letters*, 47,  
1096 e2020GL089269, <https://doi.org/10.1029/2020GL089269>, 2020.

1097 Guenther, A., Jiang, X., Shah, T., Huang, L., S. Kemball-Cook, and Yarwood, G.: Model of Emissions of Gases  
1098 and Aerosol from Nature Version 3 (MEGAN3) for Estimating Biogenic Emissions, *Air Pollution Modeling and  
1099 Its Application XXVI*, edited by: Mensink, C., Gong, W., and Hakami, A., Springer International Publishing,  
1100 Cham, 187-192 pp., 2020.

1101 Guenther, A. B., Jiang, X., Heald, C. L., Sakulyanontvittaya, T., Duhl, T., Emmons, L. K., and Wang, X.: The  
1102 Model of Emissions of Gases and Aerosols from Nature version 2.1 (MEGAN2.1): an extended and updated  
1103 framework for modeling biogenic emissions, *Geoscientific Model Development*, 5, 1471-1492, 2012.

1104 Guevara, M., Jorba, O., Soret, A., Petetin, H., Bowdalo, D., Serradell, K., Tena, C., Denier van der Gon, H.,  
1105 Kuenen, J., Peuch, V. H., and Pérez García-Pando, C.: Time-resolved emission reductions for atmospheric  
1106 chemistry modelling in Europe during the COVID-19 lockdowns, *Atmos. Chem. Phys.*, 21, 773-797, 10.5194/acp-  
1107 21-773-2021, 2021.

1108 Hess, P., and Brezowsky, H.: Katalog der Großwetterlagen Europas, Offenbach a.M., , 14 & 54, 1977.

1109 Huang, X., Ding, A., Gao, J., Zheng, B., Zhou, D., Qi, X., Tang, R., Wang, J., Ren, C., Nie, W., Chi, X., Xu, Z.,  
1110 Chen, L., Li, Y., Che, F., Pang, N., Wang, H., Tong, D., Qin, W., Cheng, W., Liu, W., Fu, Q., Liu, B., Chai, F.,  
1111 Davis, S. J., Zhang, Q., and He, K.: Enhanced secondary pollution offset reduction of primary emissions during  
1112 COVID-19 lockdown in China, *National Science Review*, 10.1093/nsr/nwaa137, 2020.

1113 Inness, A., Ades, M., Agustí-Panareda, A., Barré, J., Benedictow, A., Blechschmidt, A., Dominguez, J., Engelen,  
1114 R., Eskes, H., Flemming, J., Huijnen, V., Jones, L., Kipling, Z., Massart, S., Parrington, M., Peuch, V.-H., M, R.,  
1115 Remy, S., Schulz, M., and Suttie, M.: CAMS global reanalysis (EAC4), in, edited by: (ADS), C. A. M. S. C. A.  
1116 D. S., 2019a.

1117 Inness, A., Ades, M., Agustí-Panareda, A., Barre, J., Benedictow, A., Blechschmidt, A. M., Dominguez, J. J.,  
1118 Engelen, R., Eskes, H., Flemming, J., Huijnen, V., Jones, L., Kipling, Z., Massart, S., Parrington, M., Pench, V.  
1119 H., Razinger, M., Remy, S., Schulz, M., and Suttie, M.: The CAMS reanalysis of atmospheric composition,  
1120 *Atmospheric Chemistry and Physics*, 19, 3515-3556, 10.5194/acp-19-3515-2019, 2019b.

1121 James, P. M.: An objective classification method for Hess and Brezowsky Grosswetterlagen over Europe,  
1122 *Theoretical and Applied Climatology*, 88, 17-42, 10.1007/s00704-006-0239-3, 2007.

1123 Kelly, J. T., Bhawe, P. V., Nolte, C. G., Shankar, U., and Foley, K. M.: Simulating emission and chemical evolution  
1124 of coarse sea-salt particles in the Community Multiscale Air Quality (CMAQ) model, *Geoscientific Model  
1125 Development*, 3, 257-273, 2010.

1126 Kroll, J. H., Heald, C. L., Cappa, C. D., Farmer, D. K., Fry, J. L., Murphy, J. G., and Steiner, A. L.: The complex  
1127 chemical effects of COVID-19 shutdowns on air quality, *Nat Chem*, 12, 777-779, 10.1038/s41557-020-0535-z,  
1128 2020.

1129 Le Quéré, C., Jackson, R. B., Jones, M. W., Smith, A. J. P., Abernethy, S., Andrew, R. M., De-Gol, A. J., Willis,  
1130 D. R., Shan, Y., Canadell, J. G., Friedlingstein, P., Creutzig, F., and Peters, G. P.: Temporary reduction in daily

**Formatiert:** Schriftart: (Standard) Times New Roman, 10 Pt.

1131 global CO<sub>2</sub> emissions during the COVID-19 forced confinement, *Nature Climate Change*, 10, 647-653,  
1132 10.1038/s41558-020-0797-x, 2020.

1133 Lonati, G., and Riva, F.: Regional Scale Impact of the COVID-19 Lockdown on Air Quality: Gaseous Pollutants  
1134 in the Po Valley, Northern Italy, *Atmosphere*, 12, 264, 2021.

1135 Matthias, V., Arndt, J. A., Aulinger, A., Bieser, J., van der Gon, H. D., Kranenburg, R., Kuenen, J., Neumann, D.,  
1136 Pouliot, G., and Quante, M.: Modeling emissions for three-dimensional atmospheric chemistry transport models,  
1137 *Journal of the Air & Waste Management Association*, 68, 763-800, 10.1080/10962247.2018.1424057, 2018.

1138 Menut, L., Bessagnet, B., Siour, G., Mailler, S., Pennel, R., and Cholakian, A.: Impact of lockdown measures to  
1139 combat Covid-19 on air quality over western Europe, *Sci Total Environ*, 741, 140426,  
1140 10.1016/j.scitotenv.2020.140426, 2020.

1141 Mertens, M., Jöckel, P., Matthes, S., Nützel, M., Grewe, V., and Sausen, R.: COVID-19 induced lower-  
1142 tropospheric ozonechanges, *Environ. Res. Lett.*, in press, 10.1088/1748-9326/abf191, 2021.

1143 Petetin, H., Bowdalo, D., Soret, A., Guevara, M., Jorba, O., Serradell, K., and Garcia-Pando, C. P.: Meteorology-  
1144 normalized impact of the COVID-19 lockdown upon NO<sub>2</sub> pollution in Spain, *Atmospheric Chemistry and  
1145 Physics*, 20, 11119-11141, 10.5194/acp-20-11119-2020, 2020.

1146 Petrik, R., Geyer, B., and Rockel, B.: On the diurnal cycle and variability of winds in the lower planetary boundary  
1147 layer: evaluation of regional reanalyses and hindcasts, *Tellus Series a-Dynamic Meteorology and Oceanography*,  
1148 73, 1-28, 10.1080/16000870.2020.1804294, 2021.

1149 Rockel, B., Will, A., and Hense, A.: The Regional Climate Model COSMO-CLM(CCLM), *Meteorologische  
1150 Zeitschrift*, 17, 347-348, 2008.

1151 Schwarzkopf, D. A., Petrik, R., Matthias, V., and Quante, M.: A Ship Emission Modeling System with Scenario  
1152 Capabilities, *Atmospheric Environment X*, under review, 2021.

1153 Sharma, S., Zhang, M., Anshika, Gao, J., Zhang, H., and Kota, S. H.: Effect of restricted emissions during COVID-  
1154 19 on air quality in India, *Sci Total Environ*, 728, 138878, 10.1016/j.scitotenv.2020.138878, 2020.

1155 Solazzo, E., Bianconi, R., Pirovano, G., Matthias, V., Vautard, R., Moran, M. D., Appel, K. W., Bessagnet, B.,  
1156 Brandt, J., Christensen, J. H., Chemel, C., Coll, I., Ferreira, J., Forkel, R., Francis, X. V., Grell, G., Grossi, P.,  
1157 Hansen, A. B., Miranda, A. I., Nopmongkol, U., Prank, M., Sartelet, K. N., Schaap, M., Silver, J. D., Sokhi, R. S.,  
1158 Vira, J., Werhahn, J., Wolke, R., Yarwood, G., Zhang, J., Rao, S. T., and Galmarini, S.: Operational model  
1159 evaluation for particulate matter in Europe and North America in the context of AQMEII, *Atmospheric  
1160 Environment*, 53, 75-92, 2012.

1161 van Heerwaarden, C. C., Mol, W. B., Veerman, M. A., Benedict, I., Heusinkveld, B. G., Knap, W. H., Kazadzis,  
1162 S., Kouremeti, N., and Fiedler, S.: Record high solar irradiance in Western Europe during first COVID-19  
1163 lockdown largely due to unusual weather, *Communications Earth & Environment*, 2, 37, 10.1038/s43247-021-  
1164 00110-0, 2021.

1165 Velders, G. J. M., Willers, S. M., Wesseling, J., den Elshout, S. v., van der Swaluw, E., Mooibroek, D., and van  
1166 Ratingen, S.: Improvements in air quality in the Netherlands during the corona lockdown based on observations  
1167 and model simulations, *Atmospheric Environment*, 247, 10.1016/j.atmosenv.2020.118158, 2021.

1168